Effect of hydro-climate variation on biofilm dynamic and impact in intertidal environment

Elena Bastianon[1], Julie A. Hope[1], Robert M. Dorrell[1], Daniel R. Parsons[1]

[1] Energy and Environment Institute, University of Hull, Hull, HU6 7RX, United Kingdom

5   *Correspondence to*: Elena Bastianon (E.Bastianon@hull.ac.uk)

Abstract. Shallow tidal environments are very productive ecosystems yet are sensitive to environmental changes and sea level rise. Bio-morphodynamic control of these environments is therefore a crucial consideration; however, the effect of small-scale biological activity on large-scale cohesive sediment dynamic like tidal basins and estuaries is still largely unquantified. This study advances our understanding by assessing the influence of biotic and abiotic factors on biologically cohesive sediment

10   transport and morphology. An idealised benthic biofilm model is incorporated in a 1D morphodynamic model of tide-dominated channels. This study investigates the effect of a range of environmental and biological conditions on biofilm growth, and their feedback on the morphological evolution of the entire intertidal channel. By carrying out a sensitivity analysis of the bio-morphodynamic model, parameters like i) hydrodynamic disturbances; ii) seasonality; iii) biofilm growth rate; iv) temperature variation; and v) bio-cohesivity of the sediment, are systematically changed. Results reveal that key parameters

15   such as growth rate and temperature strongly influence the development of biofilm and are key determinants of equilibrium biofilm configuration and development, under a range of disturbance periodicities and intensities. Long-term simulations of intertidal channel development demonstrate that the hydrodynamic disturbances induced by tides play a key role in shaping the morphology of the bed, and the presence of surface biofilm increases the time to reach morphological equilibrium. In locations characterized by low hydrodynamic forces the biofilm grows and stabilizes the bed, inhibiting the transport of coarse

20   sediment (medium and fine sand). These findings suggest biofilm presence in channel beds results in intertidal channels that have significantly different characteristics in terms of morphology and stratigraphy compared abiotic sediments. It is concluded that inclusion of biocohesion in morphodynamic models is essential to predict estuary development and mitigate coastal erosion.

1. Introduction

25   Tidal inlets are some of the most sensitive systems to sea-level rise and environmental change. Their morphology is shaped and influenced by tides, waves, river discharge and associated sediment supply of marine and riverine sands and muds (Corenblit et al., 2007; De Haas et al., 2018). The availability of nutrients and sediment from the surrounding area in combination with dynamic environmental conditions, provide a favourable setting for numerous aquatic species, making them one of the most ecologically important environments (Meire et al., 2005). Even though strongly driven by abiotic processes,

30   biotic processes can determine the geomorphological evolution of intertidal areas (Defew et al., 2002; Malarkey et al., 2015; Parsons et al., 2016; Vignaga et al., 2013). In order to manage these systems and adapt for future changes, there is the need for models that are able to incorporate the role of biocohesion on geomorphology. Those currently available are not yet robust enough to predict, with confidence, very far into the future. Consequently, understanding the interactions between hydrodynamics, sediment erosion and deposition, and biological communities becomes crucial for the sustainable management

35   of estuaries and intertidal environments.

Biological activity on the seabed is known to have a significant influence on the bed composition and dynamics of cohesive and non-cohesive sediment at both small spatial and temporal scales (Decho, 2000). The presence of benthic microorganisms and the substances that they secrete strongly mediate the physical behaviour and functionality of the depositional system, influencing the structure and behaviour of sedimentary habitats, acting as ecosystem engineers (Paterson, 1997; Paterson et

40   al., 2018). Microphytobenthos (MPB) is an assemblage of microbial cells, e.g., diatoms, cyanobacteria and heterotrophic bacteria, aggregated within a gel matrix composed of a mixture of lipids, proteins and polysaccharides, known as Extracellular Polymeric Substances (EPS), that form benthic biofilms in intertidal and subtidal areas (Austin et al., 1999; Decho, 2000; Paterson et al., 1994; Tolhurst et al., 2002; Underwood and Paterson, 1993). Biofilms composed of MPB and EPS are ubiquitous in aquatic sediments (sand and mud) from shallow fluvial systems to continental shelves within the photic zone

45   (Cahoon 1999), even under physical disturbance from flow (Hope et al., 2020; Pinckney et al., 2018). While prevalence and patchiness can be greater on intertidal muddy flats, biofilm distribution in sandier intertidal and subtidal channels can be more homogenous as seen in the Western Scheldt (Daggers et al., 2020).

It has been shown that secreted EPS is crucial in the adhesion/cohesion of the substratum and sediment particles, and it can act as a protective layer at the bed surface reducing the bed roughness, influencing significantly the erosion and deposition of

50   sediment particles by raising the sediment erosion threshold due to cohesion (Tolhurst et al. 2002, Tolhurst et al. 2006, Tolhurst et al. 2009, Paterson et al., 2018, Hope et al. 2020). This promotes the sedimentation of fine-grained particles and subsequently stimulates biofilm growth (Weerman et al., 2010) as nutrient are supplied to the bed. Microbial production of EPS is influenced not only by nutrient availability, but can be stimulated with exposure to contaminants such as heavy metals and nanoparticles (Ruddy et al. 1998; Lubarksy et al., 2010; Joshi et al., 2012). Even at low EPS content (Tolhurst et al., 2002), both EPS

55   concentrations (quantity) and EPS components (quality) play important roles on the binding effect on sediment particles increasing the critical threshold for erosion and 'biostabilisation' (Paterson et al., 1989; Tolhurst et al., 2002; Widdows et al., 2000), thereby reducing sediment resuspension and bed erosion (Lubarsky et al., 2010; Malarkey et al., 2015; Parsons et al., 2016). This allows the spatial development of biofilms and stabilization across large geomorphological features (Weerman et al., 2010, Friend et al., 2008). By reducing the concentration of fine sediment resuspended and consequently the turbidity of

60   the water column, biostabilisation improves light penetration to the sediment surface, creating a positive feedback to the biofilm community and more growth. Biostabilisation also limits the resuspension of coarse particles that, by moving, could cause abrasion to the biofilm layer and the removal of large sections of biofilm from the bed (Lanuru et al., 2007). Further, the stabilization of the water-sediment interface by benthic biofilm is important for the regulation and bentho-pelagic exchange of

carbon, nitrogen and oxygen with the substrate (Cahoon 1999) and subsequently the transfer of energy and resource to adjacent habitats (Savage et al., 2012).

These processes are complicated by the presence of benthic bioturbators that disrupt and graze on MPB, and they can have a high impact on mudflat morphology because they can physically destabilise the bed (e.g. de Deckere et al. 2001, Brückner et al., 2021) and trigger sediment resuspension that is otherwise stabilized by diatoms. Furthermore, the establishment of biostabilizers might be affected by sediment destabilization and seed predation from bioturbators (Cozzoli et al., 2019). In turn, bioturbators organically enrich the sediment via biodeposition which can promote the MPB growth (e.g. Andersen et al., 2010; Donadi et al., 2013); and biostabilizers can modify the hydrodynamics and sediment properties around them (Brückner et al., 2020), impacting the size and density of bioturbators communities (Walles et al., 2015).

While microbially produced EPS is more abundant in cohesive sediment (muddy bed), studies have shown that EPS production by bacteria and microphytes can also play a significant role in non-cohesive and mixed sediment substrates by hindering bedform development and inhibiting erosion (Malarkey et al., 2015, Parsons et al., 2016, Chen et al., 2017, Hope et al., 2020). The influence of benthic biofilms and EPS on sediment erosion is widely recognized and characterised across different sedimentary habitats (e.g. Paterson, 1989; MacIntyre et al., 1996; Marani et al., 2010; Malarkey et al., 2016; Hope et al., 2020; Chen et al., 2021), but few numerical studies account for these processes. The exclusion of biocohesion and biostabilisation effects makes it difficult for predictive models of sediment stability to be sufficiently accurate. This is primarily due to the difficulty of simultaneously coupling the physical, biological and biodiversity components. Seasonal changes in environmental conditions and grazer communities can mediate biofilm grow rate (Underwood and Paterson, 2003; Montani et al., 2003; Zhang et al., 2021; Daggers et al., 2020, Brückner et al., 2021), but interannual changes in key biota, through their influence on sediment erosion, and the consequences for intertidal ecology and morphology, can also be driven by climatic factors such as changes in water and sediment temperature (Marani et al., 2007, 2010; Mariotti and Fagherazzi, 2012), which is strongly regulated by the light availability due to the turbidity of the water column. Quantifying and understanding these benthic processes in order to parameterize them into mathematical models is critical for providing insights into the relative importance of biological and physical factors in sediment erosion/accretion in the intertidal zone.

A range of hydro-morphodynamic models have attempted to parameterize eco-engineering processes on varying spatial and temporal scales (Brückner et al., 2020; Brückner et al., 2021; Coco et al., 2013; Le Hir et al., 2007; Mariotti and Canestrelli, 2017). While extensive field and flume studies are available in literature on the effect of MPB and faunal on sediment erosion (Le Hir et al. 2007, Cozzoli et al., 2019), the main challenges in modelling these types of environments are the complexity of the interaction between the different biotic and abiotic contributors, the time and spatial scales, and the fact that variation in sediment stability might reflect site-specific differences (Le Hir et al., 2007; Pivato et al., 2019). In fact, the interactions between these processes are strongly regulated by spatio-temporal conditions, (e.g. Widdows et al., 2000; Van de Lageweg et al. 2017; Paterson et al. 2018; Best et al. 2018; Cozzoli et al., 2019), making it difficult for predictive models of sediment stability to make generalities from site-specific findings and to be sufficiently accurate.

For the first time, this study investigates the effect of the environmental conditions, such as temperature, seasonality and sediment rheology, on biofilm growth and its feedback to the bed stability and morphological evolution over an entire intertidal channel. The main objective was to investigate and define the key parameters of the biofilm development model that influence the intertidal channel morphology. The combined effect of temperature, biofilm growth rate and surface biofilm removal due to tidal dynamics is investigated for different scenarios.

A one-dimensional eco-morphodynamic shallow water model is implemented and tested in this study to investigate the effect of biostabilisation due to the presence of surface biofilm. The model accounts for the effect of tidal oscillation on a non-uniform non-cohesive sediment channel subject to tidal fluctuations at the ocean boundary, and it allows to store the information of the stratigraphy of the deposit emplaced. The biofilm logistic growth model accounts for the effect of hydro-climate variation on the biofilm development, such as temperature changes and carpet-like erosion, as these are key factors controlling biofilm development (Pivato et al., 2019). The model is tested for different benthic biofilm growth rates. Biostabilisation from presence of surface biofilms is implemented in the 1D morphodynamic shallow water model assuming a linear relationship that correlates the amount of biofilm biomass with the increase of the sediment critical shear stress for erosion (Le Hir et al. 2007). The model is applied to an initial flat bed to investigate the implications of different sediment temperatures, representative of different climate scenarios, and different sediment rheology on the channel development.

1.1 Bio-sedimentology summary of processes and controls

Since the living and abiotic elements vary temporally and spatially, it is not surprising that the functions and importance of these various factors in determining sediment stability also vary (Black, 1997; Defew et al., 2002; Friend et al., 2003; Paterson et al., 1994; Riethmuller et al., 2000; Underwood et al., 1995; Yallop et al., 1994b). Benthic biofilms change the fundamental properties of sediment and bed substrate: when biofilm develops on the bed surface, it acts as a protective skin on the sediment surface inhibiting entrainment (Paterson et al., 2000) with greater volumes of biofilm required to stabilise sandier beds (Hope et al., 2020).

Numerous studies in marine intertidal environments show a positive correlation between sediment stability in terms of critical shear stress for erosion (τ_{bc}) and EPS components of biofilm. Although it is EPS that stabilises the bed, not the MPB *per se*, chlorophyll-a (Chl-a), a proxy of living MPB biomass, provides a good approximation of biostabilisation potential (Defew et al., 2002; Paterson et al., 2000; Riethmuller et al., 2000, Haro et al., 2022). Chl-a is often the preferred measurement, due to its ecological significance and the fact that it is easy to evaluate (both in the field and by optical remote sensing)(Andersen, 2001; Le Hir et al., 2007), but Chl-a – stability relationships can often be weak, emphasising the complexity of this phenomenon and that important interactions are being missed. Hydro-sedimentary processes, modulated by the shear stresses at the bed due to tidal and waves, regulate the biofilm resuspension process and its flux in the water column. The erosion fluxes depend on the bed erodibility, described by the resistance of the sediment to be eroded (Orvain et al., 2014). Changes in bed erodibility, which vary largely in space and time, is the result of a complex interaction between sediment properties, bioturbation activities, grazing, biofilms deposition, reseeding and growth rate (Wood and Widdows, 2002; Thrush et al., 2012;

130 Cozzoli et al., 2019). Due to the complexity of these systems, multiple factors play a relevant role in defining a relationship between critical shear stress for erosion and Chl-a or EPS. There is non-standard relationship but a general tendency for shear stress to increase with Chl-a content (Paterson et al., 1994; Yallop et al., 1994a; Underwood et al., 1995; Riethmuller et al., 2000; Defew et al., 2002; Friend et al., 2003; Le Hir et al., 2007; Righetti and Lucarelli, 2007; Fang et al., 2014), and often results are site specific (Riethmüller et al., 2000; Le Hir et al., 2007; Katz et al., 2018). There is thus a fundamental need for a

135 broad-scale bio-morphodynamic approach to synthesis the general effects across habitats modulated, for example, by the distribution of benthic macrofauna, the sediment types, the water content, or the tidal range.

The development of biofilm is controlled by various sedimentary characteristics, biogeochemical drivers, and light-related photosynthesis parameters (e.g. optimum and maximum temperature for MPB photosynthesis, light saturation parameter) and their spatio-temporal variability (MacIntyre et al., 1996; Pivato et al., 2019, Savelli et al., 2020), the availability of nutrients

140 (Hillebrand and Sommer, 1997), hydrodynamic disturbances such as currents and waves (Mariotti and Fagherazzi, 2012; Tolhurst et al., 2009; Tolhurst et al., 2006), and grazing benthic macrofauna (Hillebrand et al., 2000; Montserrat et al., 2008). Even when biofilms are removed during tidal inundation, the remaining MPB community can quickly re-establish itself, depending on the prevailing conditions, with a subsequent increase in biostability, as cell numbers increase and EPS secretions once again build up (Valentine et al., 2014; Chen et al., 2019; Hope et al., 2020). The prevailing environmental conditions can

145 significantly influence biostabilisation processes, with the temperature of the water and underlying sediment layers exerting a major influence on chemical and biological processes and kinetics including benthic nutrient cycling (Smith, 2002; Pivato et al., 2019). In shallow water environments, the energy exchange at the water-sediment interface, the turbidity of the water column and the light reaching the bed surface are crucial to appropriately describe the sediment temperature (Pivato et al., 2018, 2019). Experimental studies of the response of biofilm communities to water warming have shown faster biofilm growth

150 with the increase of temperature (Majdi et al., 2020). Therefore, seasonal temperature changes influence the resistance to erosion (Thom et al., 2015), for example increases in temperature during the spring, promote photosynthesis, leading to higher Chl-a concentrations and biofilm growth and greater biostabilisation (Underwood and Paterson, 1993; Savelli et al., 2018; Pivato et al., 2019; Haro et al., 2022).

When sediments are covered by biofilm, the entrainment process can occur as sediment-biofilm coated particles (flocs), or via

155 the resuspension of sediment-biofilm aggregates (biofilm failure due to carpet-like erosion) (Shang et al., 2014; Fang et al., 2016; Fang et al., 2017). Resuspended biofilm coated particles can be transported as bedload, and deposited under the different settling velocities, governed by the sediment shape and size, amount of biofilm and density of the particles or flocs (Koh et al., 2007). Hydrodynamic disturbances from currents, tides and waves play a cardinal role, eroding the biofilm and eventually detaching it from the sediment surface. Once the protective biofilm is broken or removed, the underlying clean sediment is

160 exposed, which erodibility is regulated by the characteristic sediment grain size of the substrate (Defew et al., 2002; Le Hir et al., 2007; Sutherland et al., 1998).

2. Methodology

A 1D morphodynamic model for tide-dominated channels implemented with a function that describe the surface biofilm growth was used to determine the relative importance of different bio-physical factors on the development of an intertidal channel longitudinal profile and stratigraphy. The abiotic physical processes included in this study are tidal currents, sediment erosion, transport and deposition. The model takes into account the dynamics of biofilm development and its feedback on the erosional and depositional sediment transport processes. The model is based on the one-dimensional shallow water equations (1D-SWE) for the flow mass, sediment and momentum conservation, modified according with Defina (2000) to account for partially dry areas, such as the beach that can be formed at the landward boundary of the model domain (Figure 1). The model is implemented with a procedure that stores and access the information of the grain size of the stratigraphy of the deposit.
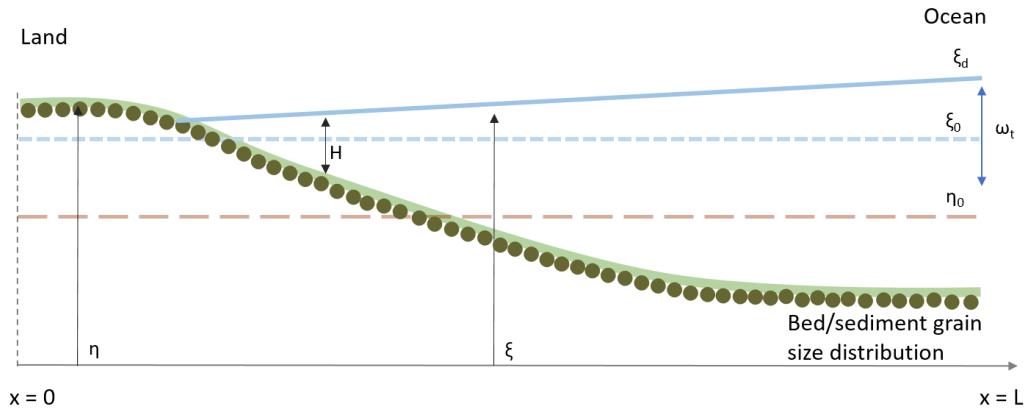
Figure 1: Schematic representation of the model geometry. The ξ and η are the water surface elevation and channel bed elevation, at the beginning of the simulation the bed is assumed horizontal (η_0), the water depth is H and the mean water surface elevation is ξ_0. ω_t represent the tidal amplitude, and the water surface elevation at the ocean boundary (x = L) is ξ_d

2.1 1D SWE model for tidal channel accounting for partially dry areas

Shallow water equations model (Chaudhry, 2008) are used to describe temporal and 1D spatial variation of idealised tidally-dominated channel reaches (Figure 1). The domain is bounded by the ocean, where the tidal oscillations are modelled as a sine curve with amplitude α_t and period ω_t. Input of riverine water and sediment at the landward boundary (Lanzoni and Seminara, 2002), and interaction of the channel with tidal flats and intertidal areas (Todeschini et al., 2008) are assumed negligible.

The shallow water equations, modified by Viparelli et al. (2019) according with Defina (2000), account for the partially dry areas such as when the channel bed is only periodically submerged. Defina (2000) derived the two-dimensional shallow water equations by averaging the Reynolds equations over the bottom irregularities; and then integrated them for mass and momentum conservation in the direction normal to the channel bed. The one dimensional form is obtained by integrating the equations in the transverse direction (Viparelli et al., 2019), giving:

$$\begin{cases} F_H \dfrac{\partial A_i}{\partial t} + \dfrac{\partial Q}{\partial x} = 0, & \text{(1a)} \\[2mm] \dfrac{\partial Q}{\partial t} + \dfrac{\partial}{\partial x}\left(\dfrac{Q^2}{A_c}\right) + \rho g A_c \dfrac{\partial \xi}{\partial x} + \dfrac{\tau_b}{\rho}\chi = 0, & \text{(1b)} \end{cases}$$

185   Where Q is the volumetric flow discharge, A_C is the cross sectional area, and ρ is the water density. The cross sectional area averaged over bed irregularities A_i is equal to $(W \cdot \xi)$, the wet fraction of the channel bed (F_H) is computed as function of the characteristic length scale of the bed irregularities $(a_r$, assumed equal to 1 cm), the effective flow depth (Y), and the average bed shear stress (τ_b) acting over the wetted perimeter χ (see Viparelli et al., 2019 for further details of the 1D morphodynamic model). The model validation is presented in Appendix 1 and shows that the model can reasonably capture the magnitude and

190   timing of the bed changes. The numerical model is demonstrated to be second order accurate and model parameters are reported in Table 1.

Table 1: Parameter for the shallow water model

Variable	Value	Description
L	25 m	Channel length
W	0.30 m	Channel width
C_f	0.009	Friction coefficient
D_g	0.3 mm	Geometric mean sediment grain size
ρ_s	2650 Kg/m^3	Density of the sediment
α_t	0.025 m	Tidal amplitude
ω	12 h	Tidal period
η_o	0.4 m	Initial bed elevation
S_f	0	Initial bed slope
ξ_o	2 m	Mean water surface elevation
N	51	Number of computational nodes

2.2 Sediment transport model

A sediment transport model is incorporated to describe well mixed, non-cohesive sediment transport and the coupled

195   morphodynmics (Viparelli et al., 2019). The total volumetric bed material load (Q_b) is calculated as the contribution of bedload and suspended load. The equations to compute the bedload and the suspended load implemented in the model have been selected to let the direct correlation between the amount of biofilm biomass on the bed, and the updated critical shear stress for sediment motion that results in biostabilisation.

The bedload is computed using the Ashida and Michiue relation, while the McLean formulation is used to model the

200   entrainment of sediment in suspension. The total material load (Q_b) is the sum of the contribution of bedload and suspended load, summed over all the grain sizes; and the volume fraction content of sediment with characteristic diameter D_i can be computed as $(Q_{b,bi} + Q_{b,si})/Q_b$.

The equation for the conservation of the sediment material coupled with a procedure to store the information of the stratigraphy of the deposit are solved to compute the temporal evolution of the bed profile (η) and the spatial distribution of the sediment size (Viparelli et al., 2010). To solve this equation, according with the Hirano active layer approximation (Hirano, 1971), the deposit can be divided into two regions, the active layer and the substrate. The active layer (L_a) is the topmost part of the deposit where the sediment particles can interact with the flow and it is assumed well mixed, so that the grain size distribution of the sediment on the active layer can change in space and time but it is assumed constant in the vertical direction. The substrate ($\eta - L_a$) is located below the active layer and does not interact with the flow; the sediment fraction in the substrate varies in space, but not in time. Exchange between the substrate and the active layer occurs in the case of aggradation and degradation. During aggradation the distance between the substrate and the active layer increases, and layers can be added to the grid for the storage of the newly deposited sediment. The grain-size distribution of the antecedent storage layer is computed a weighted average, while the sediment composition of the new storage layers has the same grain-size distribution of the newly deposited material. Interested readers may refer to Viparelli et al. (2010) for further details about the deposit storage procedure.

2.3 Biofilm-dependent erodibility

The novelty of this work is the implementation of a 1D morphodynamic model for intertidal channels with a biofilm growth model that accounts for the effect of seasonality on sediment temperature and light. This study aims to understand the general behaviour of the system and investigate the sensitivity of the biofilm model parameters on the channel development process, hence the assumption of spatially homogenous biofilm or constrain the development of biofilm only in the cells where the water depth is smaller than 0.05 m are reasonable. Once the biofilm biomass is estimated according with the biofilm growth model, the critical shear stress for erosion is updated to account for the biostabilisation. According with Le Hir et al. (2007) the increase in critical shear stress is assumed proportional to the biofilm biomass available on the bed (B, measured in mg Chl-a/m^2):

$$\tau_{bc} = \tau_{bc,0} + \alpha B, \tag{2}$$

Here ($\tau_{bc,0}$) is the critical shear stress for clean sediment. The updated value for the critical shear stress is used in the bedload and suspended load equations to correlate the sediment mobility with the amount of surface biofilm. The time evolution of biofilm biomass (B) is estimated by a simplified model proposed by Mariotti and Fagherazzi (2012) that assumes a logistic grow function for the biofilm biomass:

$$\frac{dB}{dt} = P^B B \frac{1}{1+K_B B} - \varepsilon(B - B_{min}) - E, \tag{3}$$

where P^B is the effective maximum growth rate; K_B is the half-saturation constant which represents the biofilm concentration at which it is reached half of the maximum growth rate and this term accounts for the effect of density limitation. The second term of the equation accounts for the chronic and self-generated biofilm detachment (ε: global decay parameter), not associated with the simulated hydrodynamics (e.g. senescence, heterotrophic processes, benthic macrofauna grazing), and B_{min} is the

amount of background biofilm biomass which allows the recolonization after removal. Starting from a background value for
235 the surface biofilm (B_{min}), the biofilm grows only if there are no disturbances limiting the establishment of biofilm. The last
term of the equation (3) takes into account the effect of extremely high intensity flow events (E) that are able to mobilize the
bed and completely remove the surface biofilm, exposing the clean sediment underneath. The reference values for the
parameters of the biofilm growth function (Table 2) are based on field observations, assuming that in equilibrium conditions
the surface biofilm biomass is equal to 200 mg Chl-a/m^2 (Mariotti and Fagherazzi, 2012; Le Hir et al., 2007), which is a value
240 commonly found in intertidal environments in temperate areas (Mariotti and Fagherazzi, 2012, Le Hir et al., 2007). At the
initial stages, the growth of undisturbed biofilm is approximately exponential then, as the saturation begins, it slows to linear
until it reaches maturity when the growth stops and the amount of biofilm on the bed surface remain constant for the entire
duration of the simulation, reaching asymptotically an equilibrium condition (Figure 2a).
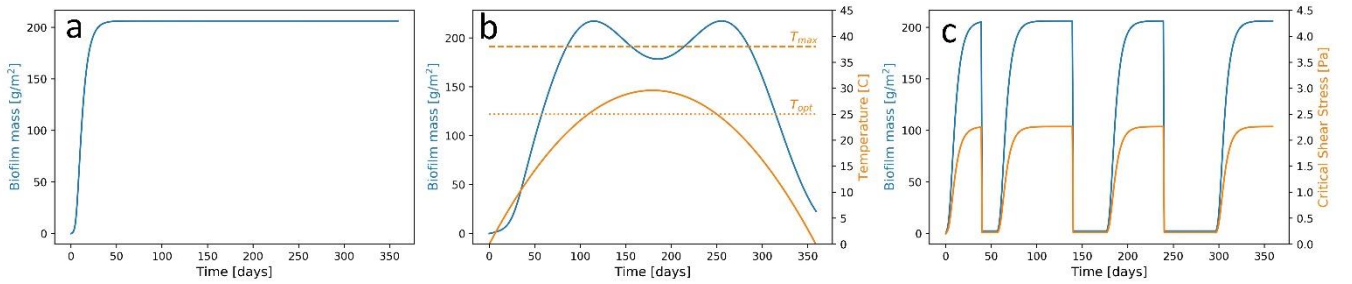
245 **Figure 2: Biofilm development in time. Biofilm growth pattern in the case of (a) annual undisturbed growing following the logistic grow function, (b) affected by the variation of sediment temperature due to seasonality over a yearlong simulation, and (c) affected by the carpet-like erosion**

The biofilm model has been implemented to account for the seasonal cycle of temperature and light as proposed by Pivato et
al. (2019), based on the vertical energy transfer within the water–sediment continuum. This sediment temperature model
250 simulates natural conditions that regulate the development of biofilm, such as the effect of winter conditions that limit the
growth of MPB, leading to lower surface sediment biostabilisation and resistance to erosion compared to late spring, summer
and early fall (Figure 2b), as confirmed also by *in situ* observations (Friend et al. 2002). The MPB photosynthesis and biofilm
development are strongly influenced by the seasonal changes of sediment temperature and light availability, which are
controlled by the water depth and turbidity. The sediment temperature model implemented in this study account for the effect
255 of seasonality, and it is based on sediment temperature parameters based on temperate environments as proposed by Guarini
et al. (2000), Pratt et al. (2014), Pivato et al. (2019) (Table 2). The maximum growth rate of MPB (P^B) is computed according
to Guarini et al. (2000):

$$P^B = P^B_{max} \tanh(H_{res}/E_k), \tag{4}$$

The light saturation parameter E_k (W m^{-2}) is assumed constant. The light availability (H_{res}) is represented by the residual solar
260 radiation reaching the bed and not reflected by the water surface albedo (A = 0.04) and it is computed as:

$$H_{res} = R_0 \, e^{-\lambda Y} \quad ; \quad R_0 = (1 - A) \, R_{sun}, \tag{5}$$

The extinction coefficient λ represent the capability of the water column to absorb the solar radiance, describing the average effect of the turbidity in the water column (Y: water depth) on radiative transfer, and R_{sun} is the solar radiation. P_{max}^B (h^{-1}) represents the growth rate under light saturation conditions, this parameter varies in time and it depends on the surface sediment temperature (T_{s0}) according to:

$$\begin{cases} \text{if } T_{S0} < T_{max}: & P_{max}^B = P_{max} \left(\frac{T_{max} - T_{s0}}{T_{max} - T_{opt}} \right)^\beta \exp \left[\beta \left(1 - \frac{T_{max} - T_{s0}}{T_{max} - T_{opt}} \right) \right], \\ \text{if } T_{S0} \geq T_{max}: & P_{max}^B = 0, \end{cases} \tag{6}$$

Function of the optimal and maximum temperature for photosynthesis ($T_{opt} = 25$ °C, and $T_{max} = 38$ °C), where the shape factor (β) is site dependent. The parameter P_{max} represents the maximum value for P_{max}^B and it is site and time dependent. The seasonal changes of the sediment temperature modulates the amount of biofilm biomass, and as a consequence, the biostabilisation of the bed (Figure 2b). For simplification, in this study, the sediment temperature will be assumed following a parabolic trend during the one-year interval (blue continuous line in Figure 2b, Pivato et al., 2019). Biomass increases exponentially at the beginning of the year, reaching its maximum when the sediment temperature is equal to the optimal temperature for photosynthesis (dotted orange line in Figure 2b, T_{opt}), during spring and fall. As the sediment temperature increases during the summer months (continuous orange line in Figure 2b), photoinhibition can occur and the biofilm biomass decreases (blue line in Figure 2b) reaching a local minimum when the sediment temperature is at its maximum and close to the maximum temperature for photosynthesis (dashed orange line in Figure 2b, T_{max}). The growth rate during these months is still sufficient to enable a fast recovery of the biofilm. As light and sediment temperature decreasing during the winter seasons, the environmental condition are less favorable for the growth of biofilm. In cases when availability of light at the bed is limited and the sediment temperature is lower than the optimal temperature for photosynthesis, surface biomass decreases.

The quantification of the removal of the surface biofilm by intense hydrodynamic forces (carpet-like erosion) occurs in a very short period of time and so it can be considered as instantaneous, and the catastrophic erosion (E) is:

$$E(B, t) = E_0(B) \sum_i \delta(t - t_i), \tag{7}$$

Where δ is the Dirac function and t_i is the time of the detachment, E_0 is the intensity of the extreme event, assumed as 'all-or-nothing' process and it can be described as a function of the shear stresses acting on the bed (τ):

$$E_0 = \begin{cases} 0 & \tau \leq \tau_{bc} \\ B - B_{min} & \tau > \tau_{bc} \end{cases}, \tag{8}$$

In the case that shear stresses due to the hydrodynamic forces (τ) are smaller or equal to the value of the sediment critical shear stress for erosion, there is no disruption of the surface biofilm. In the case that the stress on the bed exceed the critical value for erosion (τ_{bc}), the biofilm is eroded and it is reduced to the background value B_{min}, which allow establishment and growth of biofilm (Figure 2c). When biofilm is removed from the bed surface as carpet-like erosion, the resistance of the bed reduces

290 to a minimal value (Figure 2c) under the assumption of linear relationship between surface biofilm biomass and critical shear stress for erosion (Le Hir et al., 2007). This simplified model assumes that in the case of extreme hydrodynamic events, the erosion is on the order of mm-cm which is much larger than the thickness of the biofilm thickness (μm-mm). The range of values found in literature and the reference values selected here are reported in Table 2.

Table 2: Parameters' range found in literature (Mariotti and Fagherazzi, 2012; Pivato et al., 2019) and parameters' value used as
295 **reference in the model**

Parameter	Description	Range	Model Value
ε	Global decay [day^{-1}]	$\sim (0.001\text{-}0.1)\ u_*$	0.2
P_{max}	Maximum growth rate [day^{-1}]	0.0078-1.11	1.07
K_B	Half-saturation constant for biofilm growth (mg Chl-a/m^2)$^{-1}$	0.0162–0.508	0.02
B_{min}	Background biofilm [mg Chl-a/m^2]	$4.4\ 10^{-5}$-1.68	1
E_k	Light saturation parameter [W m^{-2}]		100
T_{max}	Maximum temperature for photosynthesis [°C]		38
T_{opt}	Optimal temperature for photosynthesis [°C]		25 °C
β	Shape parameter		2
A	Water surface albedo		0.04
R_{sun}	Solar irradiance reaching the water surface [Wm^{-2}]		$6.33\ 10^7$
λ	Extinction coefficient [m^{-1}]		2.0
α	Bio-cohesivity parameter [Pa/(mg Chl-a/m^2)]	0.001-0.02	0.01
$\tau_{bc,0}$	Clean sediment critical shear stress (without biofilm) [Pa]	0.05-1	0.2

The sediment mixture used for the simulations is characterized by median diameter $D_{50} = 0.323$ mm and geometric mean sediment grain size Dg = 0.303 mm.

By changing the biofilm model parameters within the range found in literature, this study investigates the sensitivity of the key biofilm model parameters on the morphological evolution of an intertidal channel (Table 3).

300 Firstly, it is presented a sensitivity analysis of the biofilm stability under different hydrodynamic disturbances characterized by periodicity (T) and intensity (τ_0, shear stress). The sensitivity analysis is performed for all the model parameters and within the range of values suggested in literature (0.6÷1.4 times the reference value suggested in literature, Table 2), by systematically changing the periodicity and intensity of the hydrodynamic disturbances to evaluate under which conditions the biofilm is stable. Then, with the objective to test the biofilm stability modulated by the effect of seasonality, it is performed a sensitivity

305 analysis of the maximum and minimum values of the parameters that are strongly affected by seasonality, like the biofilm grow rate (P^B) and the sediment temperature (T + 5 °C, T – 5 °C).

A second set of sensitivity analysis test aim to understand the bio-modulation of channel morphodynamics evolution for an idealized channel characterized by semidiurnal tidal. The results show the comparison between the impact on biostabilization for uniform and spatially varied surface biofilm under the effect of carpet-like erosion, which is regulated by the periodic

310 hydrodynamic disturbances changes in the water level at the seaward boundary due to the tidal forces, and seasonality. In the

case of combined effect of these conditions (seasonality and carpet-like erosion), it has been investigated how channel morphology changes with the variation of i) biofilm growth rate; ii) sediment temperature; and iii) sediment bio-cohesivity. The numerical simulations have been performed in the absence of an imposed input of sand from the ocean, and without riverine water and sediment at the landward boundary. It has been assumed an idealized 25 m long channel with constant width equal to 30 cm.

Table 3: Summary of the simulations performed in this study

Aim	Objective	Parameter considered
Sensitivity analysis of biofilm parament to study the biofilm stability	1. Investigate the impact of biofilm parameter on biofilm stability under different hydrodynamic disturbances characterized by periodicity (T) and intensity (τ_0, shear stress) (Figure 3)	P^B - Effective maximum growth rate for biofilm K_B - Half-saturation constant for biofilm growth ε - Biofilm global decay α - Bio-cohesivity parameter β - Shape parameter A - Albedo λ - Extinction coefficient E_k - Light saturation parameter
	2. Investigate the changes in biofilm biomass modulated by the effect of seasonality during a one-year cycle, under (i) rare and strong and (ii) frequent and weak disturbances (Figure 4)	P_{max} - Maximum growth rate T - Temperature
Sensitivity analysis of biofilm parament to study channel morphology (bed profile and substrate)	1. Investigate the effect of biofilm spatial distribution, seasonality and carpet-like erosion (Figure 5)	H - Water depth for biofilm development
	2. Investigate the effect of variation of nutrients, temperature and bio-cohesivity (Figures 6, 7, 8)	P_{max} - Maximum growth rate T – Temperature α - Bio-cohesivity parameter

3 Results

3.1 The control of hydrodynamic disturbances and biofilm model parameters on biofilm stability

The sensitivity analysis of the biofilm model parameters (Equation 2-3-4-5-6) have been investigated by systematically changing the intensity and the periodicity of the disturbances, to find the hydrodynamic conditions at which the status of the biofilm change from stable to detached (Figure 3). Mariotti and Fagherazzi (2012) have shown that biological biofilm growth parameters (P_B, K_b, ε) can affect the stability of surface biofilm in terms of the resistance of biofilm to be eroded from the bed by high intensity hydrodynamic forces, i.e. tides. The bio-cohesivity parameter that correlates the presence of surface biofilm with the increase of the bed resistance (α) results to be important in the determination of the equilibrium configuration (steady

325   biofilm). The parameters that describe the dimensionless shape factor in the equation that describes the sediment temperature (β), the effect of the light availability as the water surface albedo (A), the extinction coefficient (λ) which proxy of the water column turbidity and the light saturation parameter (E_k) do not influence the growth of biofilm under the effect of different hydrodynamic disturbances.
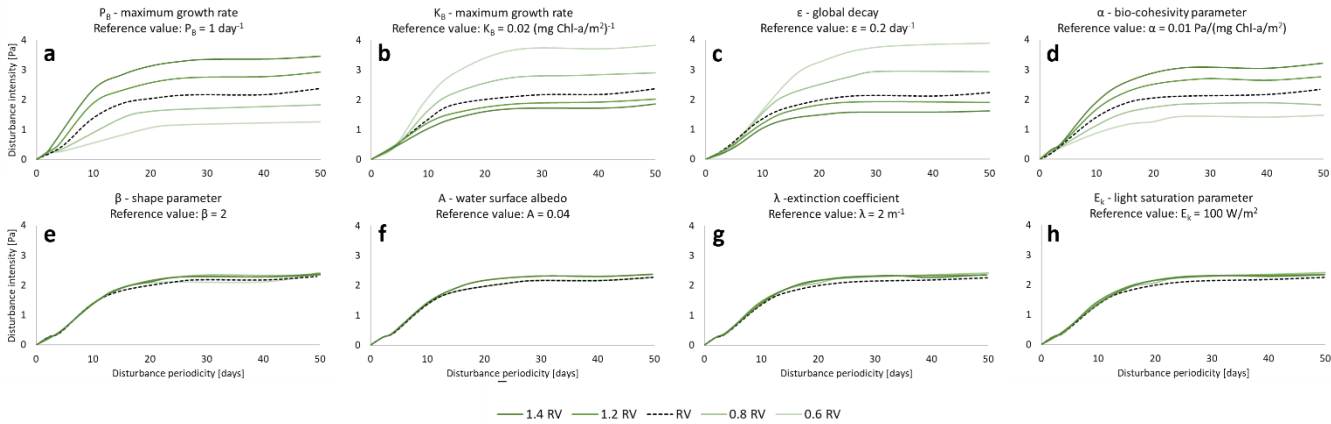
330   **Figure 3 Sensitivity analysis of the model parameters on the determination of the equilibrium configuration. The black dashed line represents the simulation considering the reference value (RV, Table 2), while dark green lines represent conditions of the parameter under examination above the reference value (1.2 and 1.4 times the reference value respectively), and light green colour represent conditions below the reference value (0.8 and 0.6 times the reference value). The area below the curves represent conditions of stable biofilm.**

335   The combined effect of seasonality of sediment temperature and hydrodynamic events are reported in Figure 4, under a set of different temperature-influenced scenarios that are intended to simulate the changes in nutrient availability in the water (growth rate parameter) and the long-term variation of temperature. The reference profile for the development of biofilm is reported in Figure 2b ($T_{s0,max}$ = 32 °C, P_B = 1.068 days^{-1}). The sensitivity analysis is carried out for a year-long cycle, the intensity and periodicity of the hydrodynamic conditions are selected from the previous analysis according with what has been observed by

340   Mariotti and Fagherazzi (2012). High-intensity and low disturbance periodicity events (case 1 in Figure 4, T = 15 days, τ_0 = 1.5 Pa) are assumed to allow the growth of biofilm under reference values for the biofilm model parameters, while under frequent and weak disturbances (case 2 in Figure 4, T = 5 days, τ_0 = 0.5 Pa) the biofilm is not fully established on the bed.
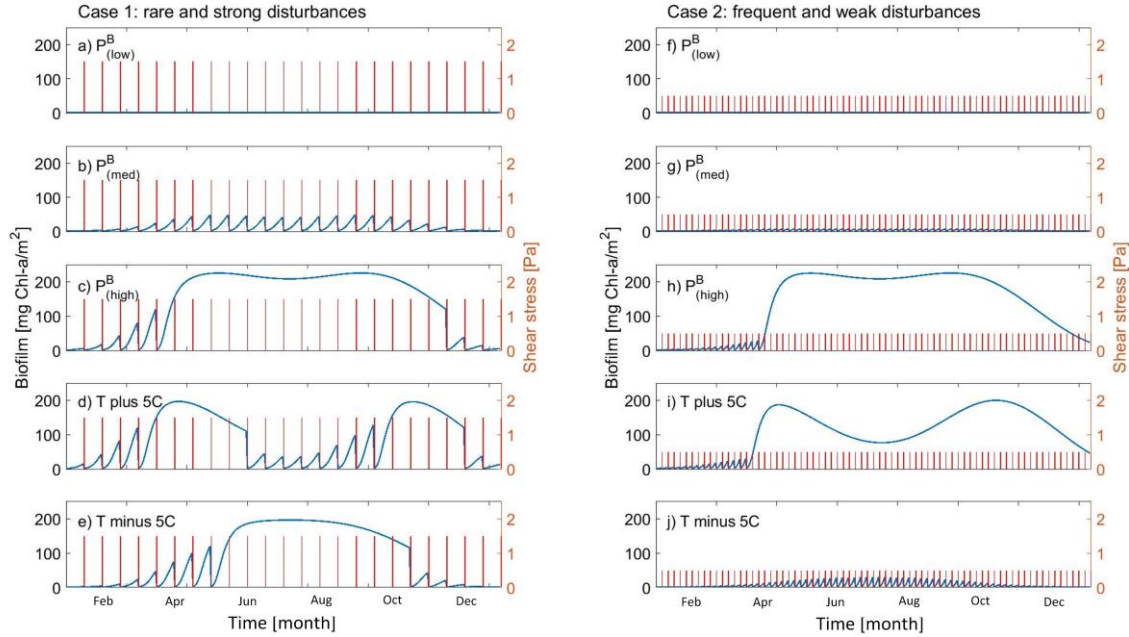
Figure 4: Effect of seasonality and hydrodynamic forces on the evolution of surface biofilm biomass. The evolution of the temperature of the sediment at the bed is simulated for a period of one year, under rare (every 15 days) and strong (1.5 Pa) hydrodynamic disturbances. The effect of different values of the growth rate parameter (panels a, b c) and sediment temperature are investigated (panels d and e). The evolution of the temperature of the sediment at the bed is simulated for a period of one year, under frequent (every 5 days) and weak (0.5 Pa) hydrodynamic disturbances. The effect of different values of the growth rate parameter (panels f, g, h) and sediment temperature are investigated (panels i and j).

With high-intensity and rare events (case 1, T = 15 days, τ_0 = 1.5 Pa), and small values of the grow rate parameter (P^B_{max} = 0.0078 and 0.5617 days^{-1}), the new settled biofilm is periodically detached by the disturbances (Figure 4a and Figure 4b). Biofilm grows during the time span between two consecutive events (Figure 4a-b), but it is destroyed every time a significant hydrodynamic event occurs. The increase in sediment resistance is not enough to prevent the erosion caused by the high-intensity events. A further increase of the maximum growth parameter (P^B_{max} = 1.068 days^{-1}) results in a more rapid growth and establishment of biofilm. During the initial and final months of the simulated year (January to mid-March, and, after mid-November) the biofilm is periodically removed, because the temperature of the sediment inhibits the development of biomass (Fig. 3c). During spring and summer months the combination of the temperature conditions and the high growth rate promote the development of stable biofilm which is able to resist the periodic disturbances.

The biofilm biomass profile under rare and intense hydrodynamic disturbances with a variation of the annual sediment temperature by ±5 °C compared with the previous simulation (P^B_{max} = 1.068 days^{-1}), is reported in Figure 4d-e. In the case of an increase of the sediment temperature the profile, analogously to the previous cases, show a slowdown of the development of biofilm in winter and fall. Furthermore, during the summer period (June to September), the sediment temperature increases above the optimal temperature for photosynthesis (T_{opt} = 25 °C) resulting in a drop in EPS production, reducing the bed

stabilization (linear decrease of the critical shear stress for erosion) and becoming more vulnerable to the hydrodynamic

365 disturbances (Fig. 3d). The effect of an overall annual reduction of the sediment temperature on biofilm is shown in Figure 4e. In this case the biofilm is more vulnerable to the disturbances at the beginning and at the end of the simulated year compared with the profile in panel c, due to the fact that temperature conditions further from the optimal temperature for photosynthesis reduces the rate of development of biofilm.

When biofilm growth rate parameter is low (Figure 4f and Fig. 3g), under frequent and weak disturbances (case 2, T = 5 days,

370 $\tau_0 = 0.5$ Pa), biofilm is periodically detached and it cannot establish during the entire simulated year. An increase of the growth rate parameter shows that in summer the biofilm can establish and cover the bed surface until the end of the year, even though the biomass decreases in fall and winter ($P^B_{max} = 1.068$ days^{-1}, Figure 4h), unlike the case of strong disturbances (panel c). The increased amount of biofilm enhanced the bed stabilization inhibiting the erosional behaviour also under further disturbances. Comparing Figure 4h with the case in which the annual sediment temperature is increased (Figure 4i) or decreased (Figure 4j)

375 by 5 °C show that an increase in temperature would decrease the amount of biomass at the bed, while a decrease of sediment temperature would not allow biofilm to establish because it would be constantly destroyed by the frequent disturbances.

It is reasonable to conclude that the presence of consolidated biofilm able to stabilize the bed does not only depend on the intensity and the frequency of the disturbing events, but also sediment temperature and seasonal parameters play a key role. The amount of biofilm biomass on the bed surface plays a significant role in defining areas of erosion, even under the same

380 hydrodynamic conditions (Mariotti and Fagherazzi, 2012; Hope et al. 2020).

3.2 Effect of seasonality and carpet-like erosion

This section explores the effects of seasonality and carpet like erosion on the morphological evolution of an intertidal channel. Two main cases are considered in this study for the spatial distribution of biofilm. One case assumes that biofilm is uniformly distributed in the entire computational domain (center column in Figure 5), to explore the case of biofilm development also in

385 the deepest portion of the channel. In fact, biostabilising organisms are found along the entire tidal range, from intertidal and subtidal areas, to shellfish reefs and on the continental shelf as it has been suggested in literature (Cahoon, 1999; Pinckney, 2018; van de Vijsel et al. 2020). For the second set of simulations, the biofilm is assumed to grow in turbid systems, where light attenuation would prevent substantial growth of surface biofilm due to the limited availability of light for the photosynthesis processes. The development of biofilm is therefore limited on locations where the water depth is below 0.05

390 m, which corresponds to the portion of the channel that experience the wet-dry transition according with the tidal amplitude range used for these simulations (right column in Figure 5).

The model is applied to investigate the separate and combine effect of carpet-like erosion and seasonality. The effect of carpet-like erosion is modulated by changes in the water level at the seaward boundary due to the tidal forces creating periodic hydrodynamic disturbances. The bed evolution after 30,000 tidal cycles are reported in Figure 5, where for the bed evolution

395 profiles the green dashed line represents the initial bed, and the blue dashed line the initial mean water surface. The profiles are compared to the final equilibrium bed profile in the case of clean sediment (Figure 5a, red dashed line). In Figure A3

(appendix) are reported the spatial distribution of the geometric mean diameter of the deposit at the end of each simulation. Initial mean diameter of the transported sediment and of the bed is 0.3 mm.

The reference case is characterized by clean sediment (Figure 5a). The model initial conditions assume a flat bed, there is a formation of an upstream migrating shore at the landward boundary due to the effect of tides at the ocean boundary, creating an alluvial deposit characterized by sediment erosion at the ocean boundary (Lanzoni and Seminara, 2002; Tambroni et al., 2005; Todeschini et al., 2008; Viparelli et al., 2019). As the shoal reaches and is impeded at the landward boundary, a beach forms and grows until conditions of morphodynamic equilibrium are met (approximately after 20,000 tidal cycles).

First, the case of spatially-uniform and stable biofilm on the bed surface for the entire duration of the simulation (Figure 5b) is modelled. This resulted in less sediment mobility compared to the clear sediment scenario (Figure 5a). The bed exhibits minor erosional behaviour at the ocean boundary, while at the land boundary the bed profile does not change in time and the bed is horizontal and stable (Figure 5c). Figure 5d shows the bed elevation in the case of water depth as constrain for the development of biofilm (H < 0.05 m). The bed is more mobile both at the ocean and landward (Figure 5d).

Clean sediment

Spatially uniform biofilm   **Biofilm where H > 0.05 m**

Stable biofilm

Seasonality

Carpet-like erosion

No. Tidal cycles

Considering the effect of seasonality (Figure 5e) there are slight increases in sediment mobility seaward (Figure 5f). While, when assuming that biofilm is present only in shallow water conditions (H < 0.05 m), it results in an increase of bed mobility (Figure 5g). Additionally, the bed needs longer time to reach equilibrium state, so it is reasonable to conclude that, even after 30,000 tidal cycles, the bed profile is still evolving.

The bed evolution in the case of surface biofilm periodically removed by the tidal induced stresses on the bed (carpet-like erosion, Figure 5h) is shown in Figure 5i. Hydrodynamic forces play a relevant role in shaping the bed, and the final profile is similar to the benchmark case, with erosion at the ocean boundary and deposition at the land boundary (Figure 5a). The presence of biofilm hinders bed evolution and more time is required to reach the equilibrium state. This is due to the periodic removal of surface biofilm due to the tidal forces, which causes periodical decreases in the bed critical shear stress for erosion and therefore biostabilisation. Assuming that biofilm is developed only under shallow water conditions (water depth smaller than 0.05 m), the channel needs even more time to reach equilibrium (Figure 5j).

For both the biofilm spatial distribution conditions investigated in this study (uniform biofilm and biofilm only in shallow water conditions, H < 0.05 m), the combined effect of seasonality and carpet-like erosion results in similar bed profile. In fact, the bed morphology is comparable in terms of bed elevation (Figure 5k and Figure 5l).

3.3 Effect of maximum biofilm growth rate parameter

Changes in the maximum growth rate in the biofilm development model (P_{max}, equation 6) result in a faster development of the biofilm, furthermore the peak of biofilm biomass appears in early stage of biofilm development (Figure 6a). In the simulations showed above (Fig. 4), the maximum growth rate parameter has been assumed equal to 1.07 day^{-1}, which is a reference value that would give a biofilm biomass of 200 mg Chl-a/m^2 in steady state conditions (Model value, Table 2). Figure 6 shows the morphology and the stratigraphy of the final bed, after 30,000 tidal cycles under different values of the biofilm grow rate parameter: small (Figure 6b and Figure 6e, P_{max} = 0.0078 day^{-1}), medium (Figure 6c and Figure 6f, P_{max} = 0.56 day^{-1}) and a large (Figure 6d and Figure 6g, P_{max} = 1.10 day^{-1}). Surface biofilm in these simulations has been assumed developing only in locations where the water depth is smaller than 0.05 m.

Small or medium values for the maximum growth parameter for biofilm create a similar final longitudinal bed profile, while for large values of P_{max} the morphology of the bed is significantly influenced by the presence of surface biofilm. In the case of small (Figure 6b) and medium (Figure 6c) values of P_{max} the final bed profiles are similar, even if smaller grow rate parameter results in a slightly higher bed mobility and the bed reaches sooner the final bed equilibrium condition. A large maximum

445 growth rate parameter influences the morphological evolution of the channel by promoting the development of surface biofilm

from the early stages of the simulation and reducing the sediment mobility (Figure 6a, green line). Under this condition, the

bed after 30,000 tidal cycles still dynamic both at the landward and seaward boundary. Overall, the grain size distribution of

the channel bed is preferentially coarse in the seaward boundary, and fine at the landward boundary. Simulations with small

values of the growth parameter result in higher sediment mobility and the deposit at the landward side is relatively coarse

450 (Figure 6e) compared with the stratigraphy of the deposit created in the case of large growth rate parameter. In this case, due

to the high stabilization, coarse fraction characterizes the bed surface at the sea boundary (Figure 6g).
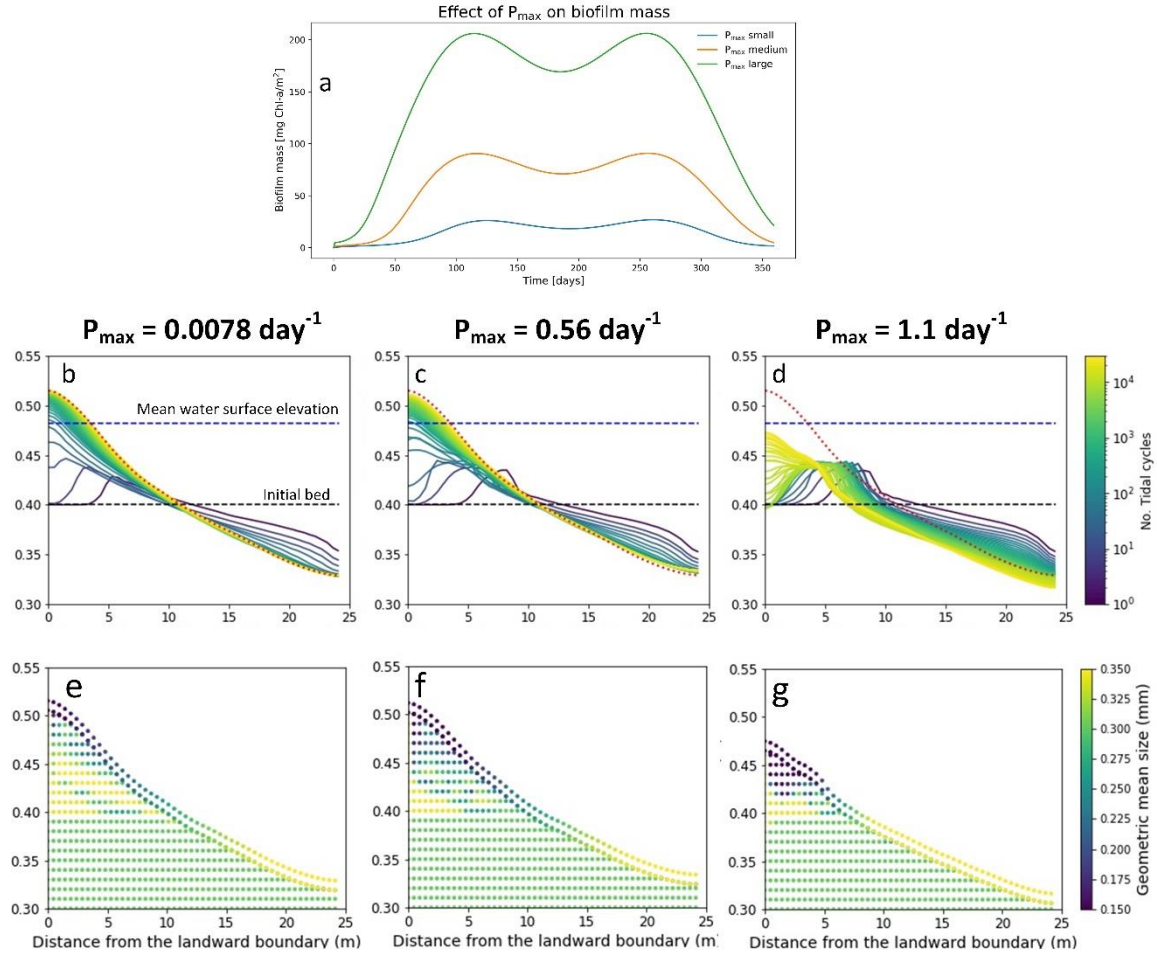
Figure 6: Effect of different values of maximum growth rate (P_{max}) on the surface biofilm biomass (a). Top row represent the bed evolution profile with small (b), medium (c) and large (d) P_{max}, after 30,000 simulated tidal cycles. The bottom row represent the
455 **geometric mean diameter of the final deposit, in the case of small (e), medium (f) and large (g) P_{max}. The bed profiles are compared with the clean sediment final bed elevation at equilibrium (red dashed lines). The blue and green dashed lines represent the initial water surface elevation and the initial bed profile respectively. Initial geometric mean size of the bed is 0.30 mm.**

3.4 Effect of temperature variation

Biofilm growth differs during the course of a year due to environmental conditions, with higher growth rate during spring and
460 beginning of summer (Thom et al., 2015; Widdows et al., 2000). The seasonality and the variation of the sediment temperature affect the development of biofilm and the consequent morphological evolution of the channel, as shown in Figure 7a. The simulations presented here focus on the effect of seasonality and changes in temperature, therefore the effect of carpet-like erosion is neglected.

The variation of the sediment temperature is function of the light availability and the turbidity of the water column. Here it is
465 assumed a sediment temperature variation of ±5°C compared to the previously simulated temperature profile, to simulate the possible scenarios in shallow water environments (Pivato et al., 2019). As mentioned before, the amount of biofilm biomass developed on the bed surface is strongly regulated by the sediment temperature (Figure 7a). Compared with the reference case (orange line), a decrease of the annual sediment temperature (T – 5°C) result in an overall slower development of biofilm, in other words it takes longer for the biofilm to reach the maximum amount of biofilm biomass at the bed (approximately 150
470 simulated days, blue line Figure 7a). In this scenario the sediment temperature does not reach the maximum temperature for photosynthesis (T_{max}) resulting in a stable biofilm biomass over a relative long period (~ between 150 and 250 days). While an increase of the annual sediment temperature (T + 5°C) would result in a more rapid development of biofilm compared with the reference case, reaching the maximum amount of surface biomass after approximately 80 simulated days (green line in Figure 7a). The sediment temperature reaches and surpasses the maximum temperature for photosynthesis (T_{max}) resulting in
475 a decrease of surface biofilm.

In the reference scenario (Figure 7a, orange line), the total amount of biofilm biomass covering the bed over the year interval is comparable to the case of low sediment temperature (Figure 7a, blue line), but these two scenarios result in a slightly different final bed profile. In the case of low sediment temperature, the bed is covered by biofilm for the period between 120 and 240 days (May – August) resulting in a more mobile bed (Figure 7b). In the reference case the bed shows presence of biofilm for
480 a longer period of time, even if it is not always at its maximum value (between 90 and 280 days), and the bed evolves more slowly (Figure 7c). An increase of temperature (Figure 7a, green line) result in high biofilm biomass around day 70 and 300, while for the rest of the year the presence of biomass on the bed is low, therefore the bed results more mobile (Figure 7d). The stratigraphy of the deposit emplaced is coarser at the ocean boundary and finer at the landward boundary after reflection for the reference case (Figure 7f), compared to the other simulated temperature conditions.
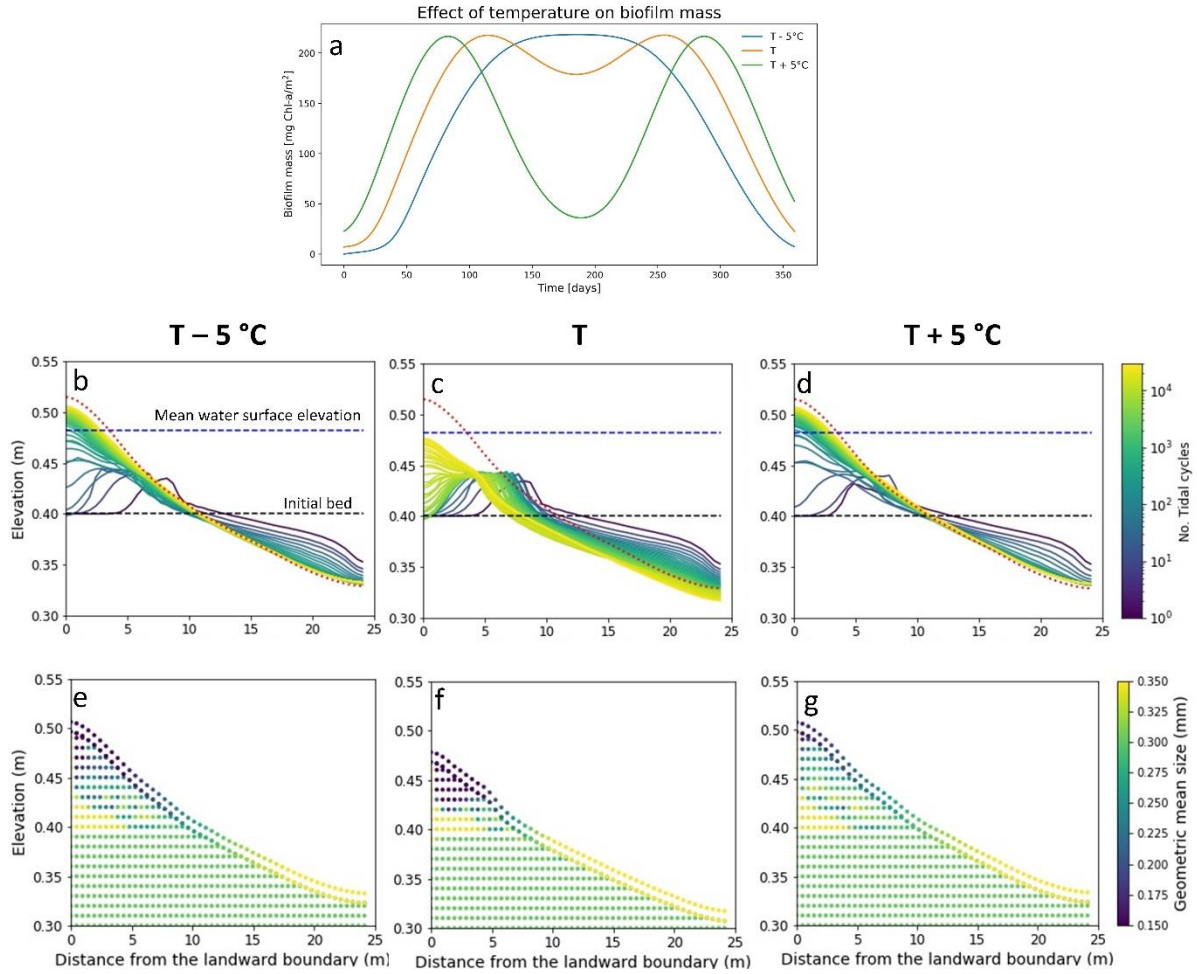
Figure 7: Effect of sediment temperature on the development of biofilm (a). Bed evolution profile (b, c, d) and final stratigraphy of the deposit (e, f, g) after 30,000 tidal cycles in the case of low sediment temperature (–5°C, left panels), reference case (center panels) and high sediment temperature (+5°C, right panels) respectively. The bed profiles are compared with the clean sediment final bed elevation at equilibrium (red dashed lines). The blue and green dashed lines represent the initial water surface elevation and the initial bed profile respectively. Initial geometric mean size of the bed is 0.30 mm.

485

490

3.5 Effect of the sediment bio-cohesivity parameter (α)

There is no universal relationship available in literature between critical shear stress for erosion (τ_{bc}) and the amount of Chl-a, considered as approximation of biostabilisation potential. This uncertainty can be explained by sediment rheology as well as different sampling techniques. Furthermore, the distribution of Chl-a content can vary spatially due to the small scale

495   morphology of the bed (Le Hir et al., 2007).

The effect of this variability has been investigated by changing the parameter (α) used to correlate the critical shear stress for erosion (τ_{bc}) with the amount of Chl-a on the bed (Eq. 2). The results of the channel morphology and stratigraphy obtained by assuming (α = 0.01) as suggested in literature (Le Hir et al., 2007; Mariotti and Fagherazzi, 2012) are compared with scenario

that account for the variability of the sediment bio-cohesivity (Figure 8). The values of the bio-cohesivity parameters tested here (α = 0.001 and 0.02) have been suggested by previous studies (Le Hir et al., 2007).

Small value of the bio-cohesivity parameter (α = 0.001) results in higher channel mobility, that is able to reach equilibrium by the end of the simulation (Figure 8a). A further increase of the bio-cohesivity parameter results in a slower morphological evolution of the channel. After 30,000 simulated tidal cycles the channel still evolving in time (Figure 8c).

For small value of the bio-cohesivity parameter, the final surface grain size distribution (Figure 8Figure d) is mostly characterized by fine sediment (D < 0.25 mm), with the coarse fraction covering the landward boundary of the domain (x < 10 m), compared with the other two cases where a larger surface area is increasingly covered by coarse material, inhibiting sediment motion (Figure 8e and Figure 8f).
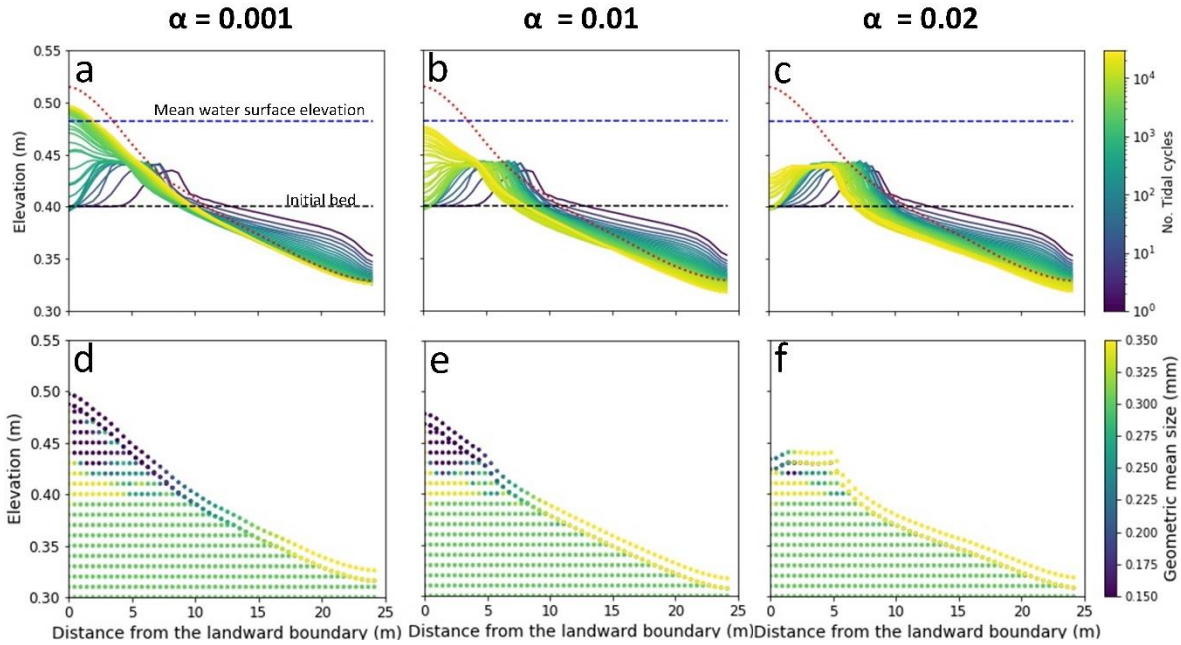
Figure 8: Effect of bio-cohesivity parameter (α) that relates the biofilm with critical shear stress for erosion. Bed evolution profile (a, b, c) and final stratigraphy of the deposit after 30,000 tidal cycles (d, e, f) in the case of α=0.001, reference case (α=0.01) and α=0.02 respectively. The bed profiles are compared with the clean sediment final bed elevation at equilibrium (red dashed lines). The blue and green dashed lines represent the initial water surface elevation and the initial bed profile respectively. Initial geometric mean size of the bed is 0.30 mm.

4 Discussion

The complex interaction between physical, chemical and biological processes and properties that govern sediment transport mechanisms are still poorly understood and quantified. It is therefore difficult for morphodynamic models to be accurate and predict into the future. Whilst some factors will be similar between estuaries, our findings confirm the need for site-specific calibration of morphodynamic models. These models must account for the contribution of different eco-engineers on tidal flat

development. Nonetheless, our investigation offers both fundamental qualitative and quantitative information regarding the
520   role of key environmental parameters in sediment stability and morphological evolution in a simplified intertidal channel.

Local hydrodynamic conditions (e.g. tides, waves) not only affect the establishment of biofilms but their recovery processes (Defew et al., 2002). Small, but frequent disturbances hinder the early stages of biofilm development, while strong disturbances can detach established biofilm (Figure 4). It is reasonable to conclude that local hydrodynamics play a crucial role in mediating the presence of biofilm, with carpet-like erosion possible when disturbance is high. Results presented in this study show that

525   in low dynamic environments where carpet-like erosion is not dominant (e.g. on bars, in central areas of tidal flats), biofilms growth is prominent (inserts of Figure 5c), resulting in a strong bio-stabilizing effect on the bed (Figure 5c). This supports field investigations where higher bed stability is observed in central tidal flats compared to the edges (Widdows at al., 2000) or differences between channels and flats (Daggers et al., 2020). Biofilm presence inhibited the sediment movement, for all shallow water habitats with low tidal forces, as demonstrated by a lack of significant changes after 30,000 tidal cycles (Figure

530   5c, d, f, g). Furthermore, deposited sediment was coarse (Figure 3Ac, d, f, g). In high dynamic environments, carpet-like erosion can remove surface biofilm exposing the clean sediment underneath and reducing biostabilisation (e.g. close to the channel, at the edge of the tidal flat), resulting in a more mobile bed profile (Figure 5i, j, k, l). Moreover, high bed shear stresses due to hydrodynamic forces (tides) can cause a general delay in biofilm formation and biostabilisation (Figure 4) and a significant decrease of the biofilm stability (Schmidt et al. 2018). This study does not incorporate the combine hydrodynamic

535   effect on surface biofilm mass of occasional storms and periodic tidal forces. Morphology and sedimentary processes on tidal flats can be strongly affected by storms and associated high-energy activities over a short time. The simulations presented in Figure 4 assumes periodic disturbances to investigate which is the effect of changes of biofilm model parameter on biofilm establishment and growth. The frequency and intensity of storms is likely to increase in the future due to climate change, and the resulting drastic morphological changes on tidal flats can occur over short durations. This will affect biofilm evolution and

540   establishment and therefore the degree of biological stabilization that occurs. Storms can induce strong wave activities, elevate water levels and cause severe erosion of tidal flats due to enhanced bed shear stress and carpet-like erosion of surface biofilm. The associated high suspended sediment concentrations and long inundation period increase the turbidity on the water column and inhibit photosynthesis. The model presented here can be easily adapted to account for the seasonal variability in storms by incorporating the combined hydrodynamic effects of occasional storms and periodic tidal forces.

545   Simulations presented here demonstrate that the biostabilising effect due to the presence of biofilm decreases the time needed for the bed to reach equilibrium compared to clean, abiotic sediment (Figure 5a). The deposits are finer than the initial bed condition at the landward boundary, which is particularly relevant as physically cohesive sediment, like mud, which facilitates saltmarsh survival and MPB growth by supplying nutrients to the bed (Smith and Underwood, 2000; Underwood 2002). The temperature model implemented in this study in turn promotes further sedimentation and can limit mud erosion(Brückner et

550   al., 2020), which is fundamental for the stabilization of wider estuarine morphological features, bank accretion and stability, predicting estuarine and deltaic development, and coastal protection. Consequently, an increasing extent and thickness of mud cover might lead to a stabilization of large-scale estuarine morphology. Although not directly modelled in this study, our

findings suggest that the sediment bed would become 'muddier' as biostabilisation is increased these changes may influence wider estuarine morphology as channels are stabilised, attract more mud and influence the evolution of channel morphology.

555 Even when trends are observed between the amount of benthic biofilm and the grain size distribution at the bed, the relationship between these two parameters is not straightforward. These relationships are strongly modulated by the role played by a complex interaction of other factors, such as the light reaching the bottom, the nutrient fluxes and human activities, and community composition of the primary producers present such as diatoms, cyanobacteria and green algae (Cahoon et al., 1999; Schmidt et al., 2018). Furthermore, in energetic and sandy sites, the frequent reworking of the substrate results in removal of

560 the biofilm and more mobile bed; while in less dynamic conditions, even small increases of fine and muddy sediment fraction can promote sediment stability (Hope et al. 2020).

In aquatic environments, spatial variability in water temperature can be natural (e.g. geothermal activity, source of water) or it can result from direct changes in local land use and activities (e.g. deforestation, industrial activities), or indirect and global changes (e.g. climate change) (Caissie, 2006; Van Vliet et al., 2011). Alteration of thermal regimes can be a major determinant

565 of changes in the diversity and resilience of aquatic biota from primary producers to consumers. The temperature model implemented in this study used surface sediment temperature as a key parameter for the growth of biofilm (Pivato et al., 2019; Pivato et al., 2018) in temperate areas (orange line in Figure 7a), and tested for ±5°C variation of temperature from the reference case. Favourable temperature conditions would result in changes in biofilm biomass production and affect fine sediment dynamics by local stabilization and accretion, reduce the turbidity in the water column, and change the hydrodynamic

570 conditions (reduce the bed roughness). In summary, the goal of these simulations was to investigate the bed morphology in colder and warmer climates, as it is reported in literature. In the first case the activity of MPB is restricted to the warmer periods (blue line in Figure 7a), while in the second case biological biomass at the bed can develop more during cooler months (green line in Figure 7a, Hope et al., 2019). Temperature regulated biofilm development at the bed strongly influence the final morphology of the channel. Dissolved oxygen levels are directly linked to water temperature, with low values of saturated

575 dissolved oxygen for higher water temperature (Pivato et al., 2019). Projected future temperature increases could thus lead to a decrease in ocean oxygen solubility and have a direct effect on organismal physiology and on biofilm development, especially in shallow water basins located in temperate regions (Kent et al., 2018). Nutrient cycling and carbon flows through benthic communities are influenced by chemical and biological processes, which are regulated by sediment temperature and light availability. Therefore, here by considering the effect of biostabilisation, this model indirectly accounts for the effect of water

580 and sediment temperature on the morphodynamic evolution of coastal shallow bays (Marani et al., 2007, 2010; Mariotti and Fagherazzi, 2012).

Biofilm growth rate and seasonality are key parameters when modelling biostabilisation (Figure 5 and Figure 6). Large variation in biostabilisation between seasons is reported in literature with the highest values in spring and the lowest in late autumn (Underwood and Paterson, 1993; Marcarelli et al., 2008; Thom et al., 2015; Schmidt et al., 2016; Waqas et al., 2020).

585 This is due to the differences in biofilm growth and composition resulting in mechanically diverse responses to the increased bed shear stress. Experiments conducted by Thom et al. (2015) reported a tenfold increase in sediment stability, depending on

boundary conditions and investigated season, and the hydrodynamic erosional process can be influenced as well by seasonality, highlighting the heterogeneity of the process. Biostabilisation is considerably higher in spring than in summer, supported by the fact that EPS protein and carbohydrate contents increase (Amos et al., 2003; Dickhudt et al., 2009; Thom et al., 2015; Schmidt et al. 2016, 2018). Seasonality also affects bed morphology, during early spring until the onset of summer, with 80% of the surface of the intertidal flats covered in biofilm, which can enhance the formation of a hummock-hollow pattern (Weerman et al., 2011a). This trend is observed in temperate humid climate (cold winters and mild summers, Figure 7a blue line, Figure 7b and e), while in warm temperate climate (mild winters and hot summers, Figure 7a green line, Figure 7d and g) the seasonal MPB biomass maximum is most likely to occur in late fall (Haro et al., 2022). Friend et al. (2003) also observed a strong seasonally dependent relationships between critical shear stress for erosion (τ_c), habitat type, Chl-a, and bed elevation, in fact the seasonal activity of the species contributes significantly in increasing or decreasing the sediment stability (Thom et al., 2015). This aspect has been parametrized in this study in the maximum growth rate parameter (P_{max}) which accounts for the effect of seasonality according to a sediment temperature model (data available in literature assume this parameter ranging between 0.0078 – 1.10 day^{-1}) (Labiod et al., 2007; Mariotti and Fagherazzi, 2012; Uehlinger et al., 1996).

Experimental and field studies have attempted to identify the roles of biological and physical processes in sediment stability using regression analyses to relate the erosion threshold to biological and physical parameters (Defew et al., 2003; Amos et al., 2004; Droppo et al., 2007; Grabowski et al., 2011). The presence of biofilm can increase bed stability up to 500% compared with non-colonized sediment (Le Hir et al., 2007; Zhu et al., 2019), and the effect of EPS are much greater than physical cohesion (Malarkey et al., 2015; Parsons et al., 2016). As Chl-a has a strong functional relationship with stabilising EPS(Friend et al., 2003; Paterson et al., 1994; Underwood et al., 1995), therefore Chl-a is often regressed against erodibility (Le Hir et al., 2007). However, there remains no universal relationship available in literature for the sediment bio-cohesivity parameter (α) that correlates the critical shear stress for erosion and Chl-a, besides the observation that the critical shear stress for erosion increases as the Chl-a content increases (Le Hir et al., 2007). Sample techniques, timing and *in-situ* versus laboratory measurement limitations play an important role in the variable relationships observed between stability and biological cohesion (Tolhurst et al., 2000a, 2000b; Le Hir et al., 2007; Perkins et al., 2003).

While remote sensing techniques can help capture spatial and temporal variability in MPB dynamics (Meleder et al., 2020; Haro et al., 2022), which is often missing from *in-situ* investigations, modelling studies, such as the current study, can help to elucidate long term changes to the bed morphology. To fully reproduce, numerically, the influence of biological cohesion in different habitats is still a challenge due to the complexity of intertidal systems and a more detailed parametrization of MPB effects is required to properly describe these complex environments (Hope et al. 2020). Significant knowledge gaps remain on how small-scale biological activity can impact large-scale cohesive sediment dynamics and overall landscape evolution. The results herein demonstrate that biophysical scale-dependent feedbacks are crucial in regulating the substrate and the spatial self-organization of intertidal ecosystems. This process is fundamental not only for understanding the development of present channels, but dating ancient biogenic deposits (van de Vijsel et al., 2020) and ancient biostabilisation processes (e.g.

620 microbialites; Burne and Moore, 1987; stromatolites; Hohl et al., 2021). Further development of the model is required to account for the long-term effect of sticky microbial biofilms on the substrate and its effect on the landscape development.

While this study provides a sensitivity analysis of the biofilm model parameters, several assumptions and simplifications of the complexity of the biogeomorphology of these environments have been made. Resuspension of MPB in the water column in highly productive ecosystems will promote the establishment of surface biofilms in adjacent habitats and settlement of MPB

625 from other. In intertidal environments, MPB, macrophytes and fauna are heterogeneously distributed, instead found in patches, though typically rather small scale. While biofilm patchiness can influence grain size of the bed, this study assumes a uniformly distributed biofilm. Similarly, macrofaunal activity can increase the bottom roughness and surface heterogeneity (Borsje et al., 2009; Coco et al., 2006; Brückner et al. 2021) enhancing the complexity of the interactions between stabilizing microbes and macrofauna. For example, infauna excrete essential nutrients which stimulates the growth of MPB and therefore bed stability

630 (Murray et al., 2014). Further, their burrows, mounds and tube mats increases the surface area of sediment, creating a patchy distribution of nutrients on the substrate enhancing the spatial complexity of biofilm distribution. These positive effects on MPB can negate the destabilizing effects of burrowing or grazing (Hope et al., 2019). The presence of grazers and the abundance of nutrients can work differently at different spatial and temporal scales, and this often creates complex interaction that are difficult quantify (Posey et al., 1999). On intertidal flats, spatial self-organisation of microbes observed during early

635 spring months can be destroyed as the season progresses. This shift towards a more homogenous surface is attributed to the presence of herbivores, bioturbation activity and the increase in grazing activity as the season progresses (Weerman et al., 2010; Weerman et al., 2011a, 2011b).

5. Conclusion

The study presented here has provided a novel insight into the biomorphodynamic evolution of intertidal channels. Biofilm

640 effects and the influence of seasonality and temperature changes on biostabilisation potential were included. The 1D biostabilisation shallow water model was implemented under different hydrodynamic conditions to investigate different climate scenarios and identify biofilm development parameters that influence the final channel morphology.

The model can be utilised to investigate the bed and deposit evolution in tidal dominated channels, starting from a horizontal bed until it reaches equilibrium. The output suggests that high hydrodynamic disturbances play a fundamental role in shaping

645 the channel equilibrium profile, by creating carpet-like erosion of the biofilm layer, which exposes the clean sediment underneath. Low hydrodynamic forces (e.g. supratidal area) allow the steady development of biofilm, and the consequent biostabilisation can inhibit sediment mobility. The frequency and intensity of the hydrodynamic disturbances, therefore regulates the growth and stability of the biofilm.

Changes in the annual sediment temperature profile (for instance due to climate change), or of the biofilm maximum growth

650 factor (regulated by e.g. nutrient availability) strongly influences the amount of surface biofilm, and as a consequence the bed

profile and stratigraphy. Increasing and decreasing the sediment temperature from the optimum for photosynthesis, both result in a less stable and less developed biofilm, and as a consequence the bed is more mobile.

It is concluded that hydrodynamic forces play a decisive role in shaping the geometry of the channel also in the uniform presence of surface biofilm, but the stratigraphy of the deposit is significantly affected by the biofilm conditions.

655

Appendix

Model Validation

The one dimensional shallow water equations modified for partially dry areas are solved simultaneously using the explicit, second-order accurate in space and time predictor-corrector MacCormack scheme (Chaudhry, 2008; Viparelli et al., 2019).

660 The numerical model is implemented on tide dominated horizontal channel subject to tidal fluctuation at the ocean boundary, which result in erosion in the ocean part and a landward migrating shoal, depositing and forming a beach until it reaches equilibrium conditions. The domain is divided into N-cells of width Δx, set equal to 0.5 m to have enough spatial resolution. The bed and water surface elevation with respect to the datum are denoted by $\eta(i)$ and $\xi(i)$ respectively.

An impermeable wall is assumed at landward boundary ($Q|_{x=0} = 0$, $Q_b|_{x=0} = 0$). An open ocean or tidal basin is assumed at the

665 ocean boundary ($x = L$) with amplitude α_t and periodicity ω_t, from where tides propagate into the domain:

$$\xi_d = \xi_0 + \alpha_t \cos(2\pi t/\omega_t), \tag{A1}$$

Extra points are added at the land and ocean boundaries of the domain to compute the predictor and corrector terms respectively, zero gradient for discharge and water surface elevation is assumed at the land boundary (x=0) while at the ocean boundary the flow rate and the water surface elevation are set equal to the value at (x=L) (Viparelli et al., 2019).

670 The final numerically modelled bed profile after 2,000 tidal cycles shows good agreement with the temporal evolution of the cross-sectional averaged bed profile Tambroni et al. (2005) obtained from laboratory investigation of the process whereby an equilibrium morphology is established in a tidal system consisting of an erodible channel connected through an inlet to a tidal sea (Figure A1). The bed profile generated from the numerical model show weaker concavity of the bed profile, resulting in better match with the theoretical predictions suggested by Seminara et al. (2010). Seminara et al. (2010) proposed two

675 theoretical predictions for tidal dominated channels, assuming Chezy coefficient as constant ($C_{constant} = 12$) or as function of the outer bottom profile at equilibrium (D_0; $C_{variable} = C_0 D_0^{1/6}$) (dashed lines in Figure A1). The numerically simulated channel slightly underestimates the bed elevation at the entrance at the landward boundary (Figure A1).
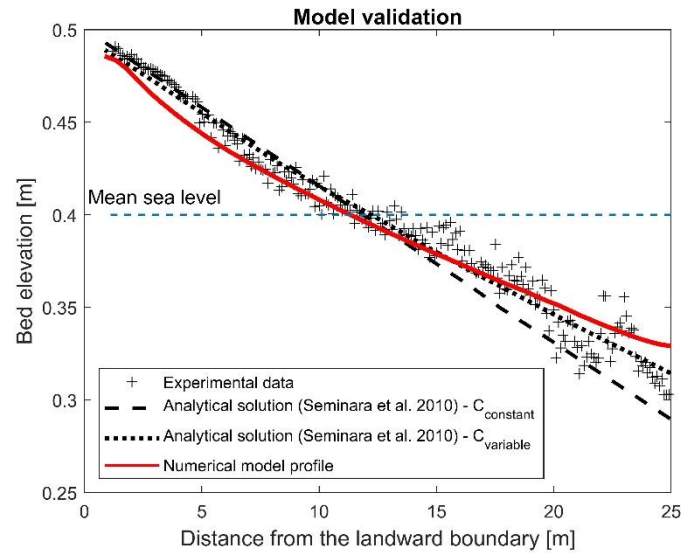
Figure A1: The experimental bed profile (grey symbols) observed by Tambroni et al. (2005) after 2000 tidal cycles in a straight, tidal channel with constant width, and the theoretical predictions (two dashed lines) resulting from equations suggested b y Seminara et al. (2010), computed with a constant and variable Chezy flow conductance, are compared with the modelled bed profile (red line)
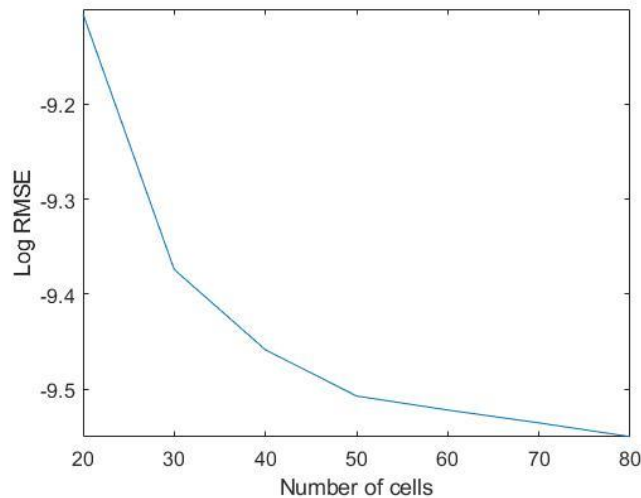
Figure A2: Logarithmic RMSE from the comparison between the model run with different number of computational cells (x axes) and the analytical solution computed with a variable Chezy flow conductance, Seminara et al. (2010)

Grid-sensitivity analysis has been performed by investigating different range of computational grid points in the streamwise direction. Increasing the grid resolution did not show any significant effect on the results (Figure A2).

Stratigraphy of the final deposit

The sediment grain size distribution of the deposit after 30,000 simulated tidal cycles is presented here.

For the reference case of clean sediment. The grain size distribution of the landward deposit associated with shoal reflection coarsened in the upward direction and from the ocean to the land (Figure A3a). Coarse sediment is transported upstream of the shoal, and is deposited in the landward part of the channel forming the coarse basal part of the deposit. As the shoal approached the landward boundary, fine sediment is deposited on the basal layer. Sediment deposited after the shoal reflection presented a fining upward profile for decreasing velocities associated with beach formation.

First, the case of spatially-uniform and stable biofilm on the bed surface for the entire duration of the simulation (Figure A3b) is modelled. The sediment mean diameter at the bed surface at the ocean boundary is coarser than the initial condition (Figure A3c). Figure A3d shows the mean diameter of the deposit emplaced with the water depth as constrain for the development of biofilm (H < 0.05 m, see section 3.2). The mean sediment diameter at the bed surface result coarser than the initial condition (0.35 mm).

Considering the effect of seasonality (Figure A3e), in the case of uniformly distributed surface biofilm, coarse sediment is found on the seabed (Figure A3f). In the case of water depth constraining the development of biofilm, coarse sediment is found at the ocean boundary, while landward the bed is characterized by finer deposit (Figure A3g).

Figure A3i and Figure A3j show the evolution of the bed with surface biofilm periodically removed by the tidal induced stresses on the bed (carpet-like erosion, Figure A3h). In both spatial distributions constrain conditions for surface biofilm, the stratigraphy of the deposit is analogous to the clear sediment case (Figure A3a), with initial coarse sediment deposited landward until the shore reflects creating a lens of fine material, after that more coarse sediment is deposited. Assuming that biofilm develop uniformly spatially, the deposit emplaced after shoal reflection at the landward boundary is coarse (Figure A3i), and the sediment at the bed is overall finer compared with the case of biofilm developing only in shallow water areas (Figure A3j). Analogous observations on the pattern of the final grain size distribution of the deposit in the case of combine effect of seasonality and carpet-like erosion can be made.

Clean sediment

Spatially uniform biofilm   **Biofilm where H > 0.05 m**

Stable biofilm

b

c

d

Seasonality

e

f

g

Carpet-like erosion

h

i

j

k

l

Geometric mean size (mm)
0.15   0.20   0.25   0.30   0.35

710
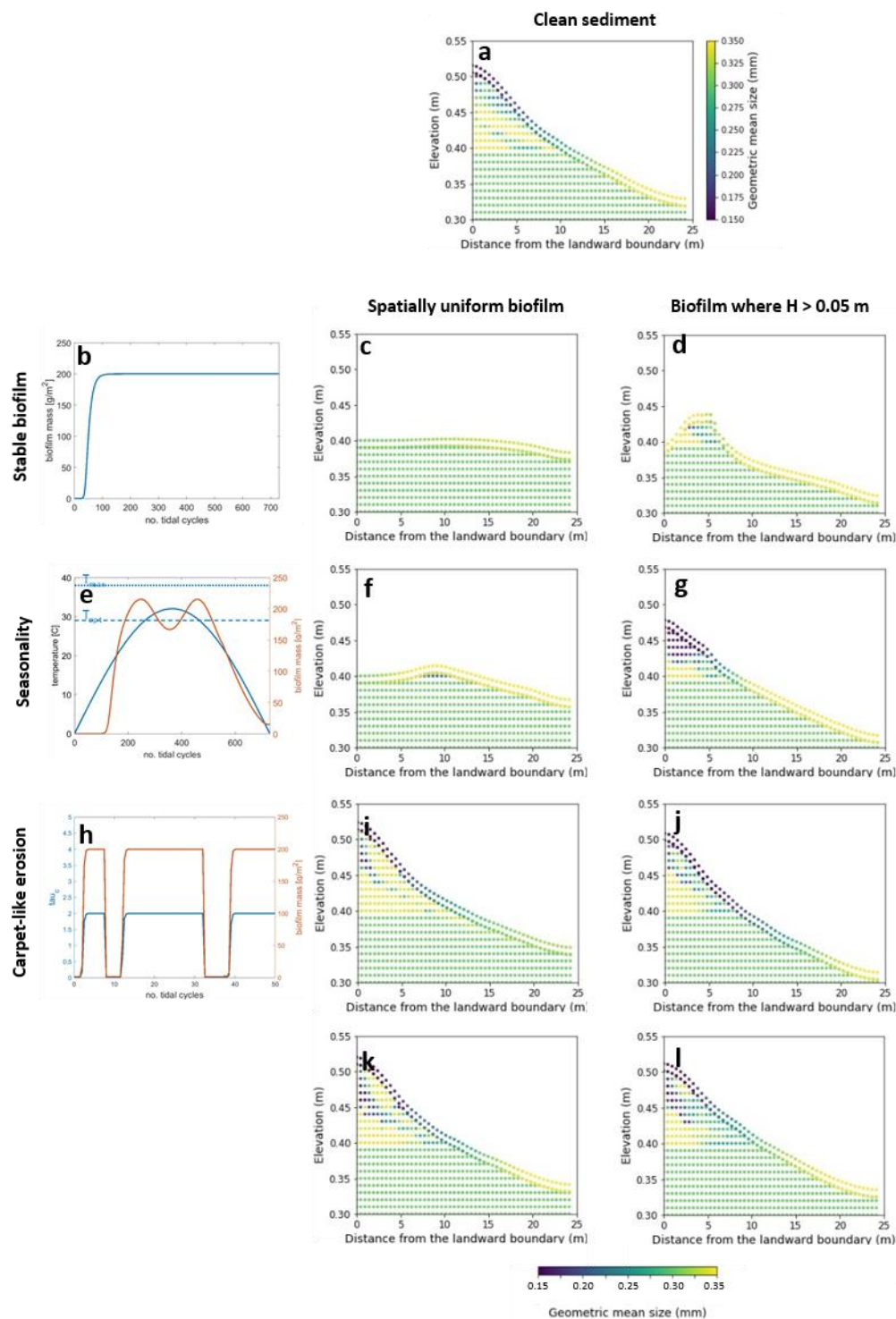
Figure A3: Final stratigraphy of the deposit after 30,000 simulated tidal cycles, under different biofilm conditions. Panel a, shows the stratigraphy of the deposit in the reference case, with clean sediment. The panels on the left column represents the time evolution of biofilm during the simulation, such as stable biofilm (panel b), effect of seasonality (panel e) and carpet-like erosion (panel h). The rows represent, respectively, the stratigraphy of the deposit under these biofilm conditions. The panels on the central column show the stratigraphy of the deposit in the case of biofilm uniformly distributed spatially. The panels on the right column show the stratigraphy of the deposit in the case of biofilm developed only in locations where the water depth is smaller than 0.05 m. Initial geometric mean size of the sediment at the bed is 0.30 mm.

715

720 **List of symbols**

A	Water surface albedo
a_r	Characteristic length scale of the bed irregularities
A_i	Cross sectional area averaged over bed irregularities (W ξ)
B	Biofilm biomass
725 B_{min}	Background biofilm
c_{0i}	Near-bed concentration of suspended sediment in the generic grain size range averaged over turbulence
C_f	Friction coefficient
c_i	Volumetric sediment concentration
D_{50}	Median diameter of the bed material
730 D_g	Geometric mean sediment grain size
D_i	Characteristic diameter
E	Catastrophic erosion
E_i	Grain size specific entrainment rate under equilibrium of suspension
E_k	Light saturation parameter
735 E_T	Entrainment rate per unit bed summed over all the grain-sizes
E_i	Entrainment rate per unit bed for each grain-size i
F_H	Wet fraction of the channel bed
g	Acceleration of gravity
H	Water depth
740 H_{res}	Light availability
K_B	Half-saturation constant for biofilm growth
L	Channel length
N	Number of computational nodes
p_i	fraction of sediment in each grain-size range
745 P^B	Effective maximum growth rate for biofilm
P_{max}	Maximum growth rate for biofilm
P_{max}^B	Biofilm growth rate under light saturation conditions
Q	Flow discharge (A_c U)
Q_b	Total material load as the sum of the contribution of bedload and suspended load summed over all the grain sizes
750 $Q_{b,bi}$	Total volumetric bed material load as the contribution of bedload, for the generic grain size i
$Q_{b,si}$	Total volumetric bed material load as the contribution of suspended load, for the generic grain size i
R	Submerged specific gravity of the bed material

	R_H	Hydraulic radius(A_c / χ)
	R_{sun}	Solar irradiance reaching the water surface
755	S_f	Friction slope
	t	Temporal coordinate
	t_i	Time detachment due to high hydrodynamic forces
	τ_b	Average bed shear stress
	T_{s0}	Surface sediment temperature
760	T_{max}	Maximum temperature for photosynthesis
	T_{opt}	Optimal temperature for photosynthesis
	U	Flow velocity
	u_{*c}	Critical shear velocity
	u_{*s}	Shear velocity due to skin friction
765	v_{si}	Fall velocity in each grain-size range
	W	Channel width
	X	Longitudinal coordinate
	Y	Effective flow depth
	α	Bio-cohesivity parameter
770	α_t	Tidal amplitude
	β	Shape parameter
	ε	Global decay
	δ	Dirac function
	η	Bed profile
775	η_o	Initial bed elevation
	λ	Extinction coefficient
	ξ	Mean water surface elevation
	ρ_s	Density of the sediment
	τ_b	Bed shear stress
780	τ_{bc}	Critical shear stress for erosion
	$\tau_{bc,0}$	Clean sediment critical shear stress
	τ_{bs}	Bed shear stress due to skin friction
	τ_i^*	Grain size specific Shields number
	$\tau_{bc,i}^*$	Grain size specific reference Shields number for significant bedload transport
785	χ	Wetted perimeter
	ω_t	Tidal period

ζ = z/b; dimensionless upward normal coordinate

Author contributions

EB developed the model, EB and DRP designed the numerical simulations; EB, RMD and JAH contributed to interpretation
790   of the results. EB drafted the manuscript, all authors contributed in editing the manuscript.

Competing interests

The authors declare that they have no conflict of interest.

References

Amos, C. L., Droppo, I. G., Gomez, E. A., and Murphy, T. P.: The stability of a remediated bed in Hamilton Harbour, Lake Ontario, Canada, Sedimentology, 50(1), 149-168, https://doi.org/10.1046%2Fj.1365-3091.2003.00542.x, 2003.

Amos, C. L., Bergamasco, A., Umgiesser, G., Cappucci, S., Cloutier, D., DeNat, L., Flindt, M., Bonaldi, M., and Cristante, S.: The stability of tidal flats in Venice Lagoon – the results of in-situ measurements using two benthic, annular flumes, Journal of Marine Systems 51, 211–241. https://doi.org/10.1016/j.jmarsys.2004.05.013, 2004.

Andersen, T. J. : Seasonal Variation in Erodibility of Two Temperate, Microtidal Mudflats, Estuarine, Coastal and Shelf Science, 53(1), 1-12, https://doi.org/10.1006/ecss.2001.0790, 2001.

Andersen, T. J., Lanuru, M., van Bernem, C., Pejrup, M., and Riethmueller, R.: Erodibility of a mixed mudflat dominated bymicrophytobenthos andCerastoderma edule, East Frisian Wadden Sea, Germany, Estuar. Coast. Shelf Sci. 87, 197–206, https//doi.org/10.1016/j.ecss.2009.10.014, 2010.

Austin, I., Andersen, T. J., and Edelvang K.: The influence of benthic diatoms and invertebrates on the erodibility of an intertidal mudflat, the Danish Wadden Sea, Estuarine, Coastal and Shelf Science, 49, 99-111, https://doi.org/10.1006/ecss.1998.0491, 1999.

Best, Ü. S., Van der Wegen, M., Dijkstra, J., Willemsen, P., Borsje, B., and Roelvink, D. J.: Do salt marshes survive sea level rise? Modelling wave action, morphodynamics and vegetation dynamics, Environmental modelling & software 109, pp. 152–166. doi:https://doi.org/10.1016/j.envsoft. 2018.08.004, 2018

Black, K. S., Microbiological factors contributing to the erosion resistance in natural cohesive sediments, Wiley, Chichester, 1997.

Borsje, B.W., de Vries, M.B., Bouma, T.J., Besio, G., Hulscher, S.J.M.H., and Herman, P.M.J.: Modeling bio-geomorphological influences for offshore sandwaves. Continental Shelf Research, 29(9), 1289–1301, https://doi.org/10.1142/9789814277426_0367, 2009.

Brownlie, W. R.: Prediction of flow depth and sediment discharge in open channels, Laboratory of Hydraulics and Water Resources, California Institute of Technology, Pasadena, California, USA, 1981.

Brückner, M. Z. M., Braat, L., Schwarz, C., and Kleinhans, M. G.: What Came First, Mud or Biostabilizers? Elucidating Interacting Effects in a Coupled Model of Mud, Saltmarsh, Microphytobenthos, and Estuarine Morphology, Water Resources Research, 56(9), https://doi.org/10.1029/2019WR026945, 2020.

Brückner, M. Z. M., Schwarz, C., Coco, G., Baar, A., Boechat Albernaz, M., and Kleinhans, M. G., Benthic species as mud patrol - modelled effects of bioturbators and biofilms on large-scale estuarine mud and morphology. Earth Surface Process. Landforms; 46:1128–1144, https://doi.org/10.1002/esp.5080, 2021.

Burne RV, and Moore L.S., Microbialites: organosedimentary deposits of benthic microbial communities. Palaios 2(3): 241–254, https://doi.org/ 10.2307/3514674, 1987.

Cahoon, L., The role of benthic microalgae in neritic ecosystems, Oceanography and marine biology, 37, 47–86, 1999.

Cahoon L.B., Nearhoof, J.E., and Tilton, C. L., Sediment Grain Size Effect on Benthic Microalgal Biomass in Shallow Aquatic Ecosystems, Estuaries, 22, 735-741, https://doi.org/10.2307/1353106, 1999.

830   Chaudhry, M. H., Open-Channel Flow, Second Edition, Springer 523 pp., 2008.

Chen, X. D., Zhang, C. K., Paterson, D. M., Thompson, C. E. L., Townend, I. H., Gong, Z., Zhou, Z., and Feng, Q., Hindered erosion: The biological mediation of noncohesive sediment behavior, Water Resources Research, 53, 4787–4801,http://doi.org/10.1002/2016WR020105, 2017.

Chen, X., Zhang, C.K., Paterson, D.M., Townend, I.H., Jin, C., Zhou, Z., Gong, Z., and Q. Feng. The effect of cyclic variation
835   of shear stress on non-cohesive sediment stabilization by microbial biofilms: the role of "biofilm precursors', Earth Surf. Proc. Land., 44: 1471-1481, 2019.

Chen, X., Zhang, C., Townend, I. H., Paterson, D. M., Gong, Z., Jiang, Q., Feng, Q., and Yu, X., Biological Cohesion as the Architect of Bed Movement Under Wave Action. Geophysical Research Letters, 48(5), e2020GL092137. https://doi.org/10.1029/2020GL092137, 2021

840   Coco, G., Thrush, S.F., Green, M.O., and Hewitt, J.E., Feedbacks between bivalve density, flow, and suspended sediment concentration on patch stable states. Ecology, 87(11), 2862–2870, https://doi.org/10.1890/0012-9658(2006)87[2862:FBBDFA]2.0.CO;2, 2006

Coco, G., Zhou, Z., van Maanen, B., Olabarrieta, M., Tinoco, R., and Townend, I., Morphodynamics of tidal networks: Advances and challenges, Marine Geology, 346, 1-16, https://doi.org/10.1016/j.margeo.2013.08.005, 2013.

845   Corenblit, D., Tabacchi, E., Steiger, J., and Gurnell, A. M., Reciprocal interactions and adjustments between fluvial landforms and vegetation dynamics in river corridors: a review of complementary approaches, Earth-Science Reviews, 84(1-2), 56-86, https://doi.org/10.1016/j.earscirev.2007.05.004, 2007.

Cozzoli, F., Gjoni, V., Del Pasqua, M., Hu, Z., Ysebaert, T., Herman, P. M., and Bouma, T. J., A process based model of cohesive sediment resuspension under bioturbators' influence, Science of the total environment, 670, 18–30,
850   https://doi.org/10.1016/j.scitotenv.2019.03.085, 2019.

Daggers, T. D., Herman, P. M. J., and van der Wal, D., Seasonal and Spatial Variability in Patchiness of Microphytobenthos on Intertidal Flats From Sentinel-2 Satellite Imagery. Frontiers in Marine Science, 7(June), 1–14. https://doi.org/10.3389/fmars.2020.00392, 2020.

De Haas, T., Pierik, H., Van der Spek, A., Cohen, K., Van Maanen, B., and Kleinhans, M., Holocene evolution of tidal systems
855   in The Netherlands: Effects of rivers, coastal boundary conditions, ecoengineering species, inherited relief and human interference, Earth-Science Reviews, 177, 139-163, https://doi.org/10.1016/j.earscirev.2017.10.006, 2018.

Decho, A. W., Microbial biofilms in intertidal systems: an overview, Continental Shelf Research, 20, 1257–1273, https://doi.org/10.1016/S0278-4343(00)00022-4, 2000.

Defew, E. C., T. J. Tolhurst, and D. M. Paterson, Site-specific features influence sediment stability of intertidal flats, Hydrology and Earth System Sciences 6, 971-981, https://doi.org/10.5194/hess-6-971-2002, 2002.

Defew, E.C., Tolhurst, T.J., Paterson, D.M., and Hagerthey, A.: Can the stability of intertidal sediments be predictedfrom proxy parameters? An in situ investigation. Estuarine and Coastal Sciences Association, Coastal Zone Topics 5,61–70, https://ueaeprints.uea.ac.uk/id/eprint/28911, 2003.

Defina, A.: Two-dimensional shallow flow equations for partially dry areas, Water Resources Research, 36(11), 3251-3264, https://doi.org/ 10.1029/2000WR900167, 2000.

Dickhudt, P. J., Friedrichs, C. T., Schaffner, L. C., and Sanford, L. P., Spatial and temporal variation in cohesive sediment erodibility in the York River estuary, eastern USA: A biologically influenced equilibrium modified by seasonal deposition, Marine Geology, 267(3), 128-140, https://doi.org/10.1016/j.margeo.2009.09.009, 2009.

Donadi, S., van der Heide, T., van der Zee, E. M., Eklof, J. S., van de Koppel, J., Weerman, E. J., Piersma, T., Olff, H., and Eriksson, B. K.: Cross-habitat interactions among bivalve species control community structure on intertidal flats. Ecology 94, 489–498, https://doi.org/ 10.1890/12-0048.1, 2013.

Droppo, I.G., Ross, N., Skafel, M., and Liss, S.N.: Biostabilisation of cohesive sediment beds in a freshwater wave-dominated environment. Limnol. Oceanogr. 52, 577–589, https://doi.org/ 10.4319/lo.2007.52.2.0577, 2007.

Fang, H. W., Shang, Q. Q., Chen, M. H., and He, G. J.: Changes in the critical erosion velocity for sediment colonized by biofilm. Sedimentology, 61(3), 648–659, https://doi.org/10.1111/sed.12065, 2014.

Fang, H. W., Fazeli, M., Cheng, W., and Dey, S.: Transport of biofilm-coated sediment particles, Journal of Hydraulic Research, 54(6), 631–645, http://doi.org/10.1080/00221686.2016.1212938, 2016.

Fang, H. W., Lai, H. J., Cheng, W., Huang, L., and He, G. J.: Modeling sediment transport with an integrated view of the biofilm effects, Water Resources Research, 53, 7536–7557, http://doi.org/10.1002/2017WR020628, 2017.

Friend, P. L., Ciavola, P., Cappucci, S., and Santos, R.: Biodependent bed parameters as a proxy tool for sediment stability in mixed habitat intertidal areas, Continental Shelf Research (23), 1899-1917, https://doi.org/ 10.1016/j.csr.2002.12.001, 2003.

Friend, P. L., Lucas, C. H., Holligan, P. M., and Collins, M. B.: Microalgal mediation of ripple mobility. Geobiology, 6(1), 70–82 , https://doi.org/ 10.1111/j.1472-4669.2007.00108.x, 2008.

Grabowski, R. C., Droppo, I. G., and Wharton, G.: Erodibility of cohesive sediment: The importance of sediment properties. Earth-Science Reviews, 105(3-4), 101–120, https://doi.org/10.1016/j.earscirev.2011.01.008, 2011

Guarini, G. F. Blanchard, P. Gros, D. Gouleau, and C. Bacher: Dynamic model of the short-term variability of microphytobentic biomass on temperate intertidal mudflats, Marine Ecology Progress Series, 195, 291-303, https://doi.org/10.3354/meps195291, 2000.

Hakvoort, J. H. M., Heineke, M., Heymann, K., Kühl, H., Riethmüller, R., and Witte, G.: A basis for mapping the erodibility of tidal flats by optical remote sensing, Marine Freshwater Research, 49(867-873), https://doi.org/10.1071/MF97090, 1998.

Haro, S., Jesus, B., Oiry, S., Papaspyrou, S., Lara, M., González, C. J., and Corzo, A.: Microphytobenthos spatio-temporal dynamics across an intertidal gradient using Random Forest classification and Sentinel-2 imagery. Science of The Total Environment, 804, 149983. https://doi.org/10.1016/j.scitotenv.2021.149983, 2022.

Hillebrand, H., and Sommer, U.: Response of epilithic microphytobenthos of the western Baltic Sea to in situ experiments with nutrient enrichment, Marine Ecology Progress Series, 160, 35-46, https://doi.org/10.3354/meps160035, 1997.

Hillebrand, H., Worm, B., and Lotze, H.: Marine microbenthic community structure regulated by nitrogen loading and grazing pressure, Marine Ecology-progress Series - MAR ECOL-PROGR SER, 204, 27-38, https://doi.org/10.3354/meps204027, 2000.

Hirano, M.: River-bed degradation with armoring, Proceedings of the Japan Society of Civil Engineers, 1971(195), 55-65, https://doi.org/10.2208/jscej1969.1971.195_55, 1971.

Hohl, S. V., and Viehmann, S.: Stromatolites as geochemical archives to reconstruct microbial habitats through deep time: Potential and pitfalls of novel radiogenic and stable isotope systems. Earth-Science Reviews, 218, 103683. https://doi.org/10.1016/j.earscirev.2021.103683, 2021.

Hope, J. A., Paterson, D. M., and Thrush, S. F.: The role of microphytobenthos in soft-sediment ecological networks and their contribution to the delivery of multiple ecosystem services. Journal of Ecology; 108:815–830.https://doi.org/10.1111/1365-2745.13322, 2019.

Hope, J. A., Malarkey, J., Baas, J. H., Peakall, J., Parsons, D. R., Manning, A. J., Bass, S. J., Lichtman, I. D., Thorne, P. D., Ye, L., and Paterson, D. M.: Interactions between sediment microbial ecology and physical dynamics drive heterogeneity in contextually similar depositional systems. Limnology and Oceanography, 65(10): 2403-2419, https://doi.org/10.1002/lno.11461, 2020

Katz, S., Segura, C., and Warren, D.: The influence of channel bed disturbance on benthic Chlorophyll a: A high resolution perspective. Geomorphology. 305. https://doi.org/10.1016/j.geomorph.2017.11.010, 2018.

Kent, A. G., Garcia, C. A., and Martiny, A. C.: Increased biofilm formation due to high-temperature adaptation in marine Roseobacter, Nature microbiology, 3(9), 989-995, https://doi.org/10.1038/s41564-018-0213-8, 2018.

Kim, B., Lee, J., Noh, J., Bae, H., Lee, C., Ha, H. J., Hwang, K., Kim, D.U., Kwon, B.O., Ha, H.K., Pierre, G., Delattre, C., Michaud, P., and Khim, J. S.: Spatiotemporal variation of extracellular polymeric substances (EPS) associated with the microphytobenthos of tidal flats in the Yellow Sea. Marine Pollution Bulletin; 171(1):112780. https://doi.org/10.1016/j.marpolbul.2021.112780, 2021.

Koh, C.H., Khim, J.S., Araki, H., Yamanishi, H., and Kenichi, K.: Within-day and seasonal patterns of microphytobenthos biomass determined by co-measurement of sediment and water column chlorophylls in the intertidal mudflat of nanaura. Estuar. Coast. Shelf Sci. 72, 42–52. https://doi.org/10.1016/j.ecss.2006.10.005, 2007.

Labiod, C., Godillot, R., and Caussadea, B.: The relationship between stream periphyton dynamics and near-bed turbulence in rough open-channel flow, Ecological Modelling, 209, https://doi.org/10.1016/j.ecolmodel.2007.06.011, 2007.

925 Lanuru, M., Riethmuller, R., van Bernem, C. and Heymann, K.: The effect of bedforms (crest and trough systems) on sediment erodibility on a back-barrier tidal flat of the East Frisian Wadden Sea, Germany. Estuar. Coastal Shelf Sci. 72, 603–614, https://doi.org/10.1016/j.ecss.2006.11.009, 2007

Lanzoni, S., and Seminara, G.: Long-term evolution and morphodynamic equilibrium of tidal channels. J. Geophys. Res. 107 (C1), 3001. https://doi.org/10.1029/2000JC00468, 2002.

Le Hir, P., Monbet, Y., and Orvain, F.: Sediment erodability in sediment transporti modeling: can we account for biota effects?
930 , Continental Shelf Research, 27, 1116-1143, https://doi.org/10.1016/j.csr.2005.11.016, 2007.

Lubarsky, H. V., Hubas, C., Chocholek, M., Larson, F., Manz, W., Paterson, D. M., and Gerbersdorf, S.: The stabilisation potential of individual and mixed assemblages of natural bacteria and microalgae, PLoS ONE, 5(11), https://doi.org/10.1371/journal.pone.0013794, 2010.

Lundkvist, M., Grui, M., Friend, P. L., and Flindt, M. R.: The relative contributions of physical and microbiological factors to
935 cohesive sediment stability. Continental Shelf Research 27, 1143–1152. https://doi.org/10.1016/J.CSR.2006.01.021, 2007

MacIntyre, H., Geider, R., and Miller, D.: Microphytobenthos: The Ecological Role of the "Secret Garden" of Unvegetated, Shallow-Water Marine Habitats. I. Distribution, Abundance and Primary Production, Estuaries and Coasts, 19, 186-201, https://doi.org/10.2307/1352224, 1996

Majdi, N., Uthoff, J., Traunspurger, W., Laffaille, P., and Maire, A.: Effect of water warming on the structure of biofilm-
940 dwelling communities, Ecological Indicators, 117, 106622, https://doi.org/10.1016/j.ecolind.2020.106622, 2020.

Malarkey, J., Baas, J. H., Hope, J.A., Aspden, R.J., Parsons, D.R., Peakall, J., Paterson, D.M., Schindler, R.J., Ye, L., Lichtman, L.D., Bass, S.J., Davies, A.G., Manning, A.J., and Thorne, P.D.: The pervasive role of biological cohesion in bedform development, Nature Communications, 6, 6257, https://doi.org/10.1038/ncomms7257, 2015.

Marani M., D'Alpaos A., Lanzoni S., Carniello L., and Rinaldo, A.: Biologically-controlled multiple equilibria of tidal
945 landforms and the fate of the Venice lagoon. Geophysical Research Letters 34(11):L11402. https://doi:10.1029/2007GL030178, 2007.

Marani, M., D'Alpaos, A., Lanzoni, S., Carniello, L., and Rinaldo, A.: The importance of being coupled: Stable states and catastrophic shifts in tidal biomorphodynamics, Journal of Geophysical Research: Earth Surface, 115(F4), https://doi.org/10.1029/2009JF001600, 2010.

950 Marcarelli, A. M., Bechtold, H. A., Rugenski, A. T., and Inouye, R. S.: Nutrient limitation of biofilm biomass and metabolism in the Upper Snake River basin, southeast Idaho, USA. Hydrobiologia, 620(1), 63–76. https://doi.org/10.1007/s10750-008-9615-6, 2008

Mariotti, G., and Fagherazzi, S.: Modeling the effect of tides and waves on benthic biofilms, Journal of Geophysical Research, 117(G04010), https://doi.org/10.1029/2012JG002064, 2012.

955   Mariotti, G., and Canestrelli, A.: Long-term morphodynamics of muddy backbarrier basins: Fill in or empty out?, Water Resources Research, 53(8), 7029-7054, https://doi.org/10.1002/2017wr020461, 2017.

Meire, P., Ysebaert, T., Van Damme, S., Van den Bergh, E., Maris, T., and Struyf, E.: The Scheldt estuary: A description of a changing ecosystem, Hydrobiologia, 540, 1-11, https://doi.org/10.1007/s10750-005-0896-8, 2005.

Méléder, V., Savelli, R., Barnett, A., Polsenaere, P., Gernez, P., Cugier, P., Lerouxel, A., Le Bris, A., Dupuy, C., Le Fouest,
960   V., Lavaud, J., 2020. Mapping the Intertidal Microphytobenthos Gross Primary Production Part I: Coupling Multispectral Remote Sensing and Physical Modeling. Frontiers in Marine Science 7.

Montani, S., Magni, P., and Abe, N.: Seasonal and interannual patterns of intertidal microphytobenthos in combination with laboratory and areal production estimates. Marine Ecology Progress Series, 249, 79–91. https://doi.org/10.3354/meps249079, 2003

965   Montserrat, F., Van Colen, C., Degraer, S., Ysebaert, T., and Herman, P.: Benthic community-mediated sediment dynamics, Marine Ecology Progress Series, 372, 43-59, https://doi.org/10.3354/meps07769, 2008.

Murray, F., Douglas, A., and Solan, M.: Species that share traits do not necessarily form distinct and universally applicable functional effect groups. Marine Ecology Progress Series, 516, 23–34. https://doi.org/10.3354/meps11020, 2014

Noffke N.: Turbulent lifestyle: microbial mats on Earth's sandy beaches – today and 3 billion years ago. GSA Today 18(10):
970   4–9. https://doi.org/10.1130/GSATG7A.1, 2008

Noffke N, Christian D, Wacey D, and Hazen RM.: Microbially induced sedimentary structures recording an ancient ecosystem in the ca. 3.48 billion-year-old Dresser Formation, Pilbara, Western Australia. Astrobiology 13(12): 1103–1124, https://doi.org/ 10.1089/ast.2013.1030, 2013.

Orvain, F., Guizien, K., Lefebvre, S., Bréret, M., and Dupuy, C.: Relevance of macrozoobenthic grazers to understand the
975   dynamic behavior of sediment erodibility and microphytobenthos resuspension in sunny summer conditions. Journal of Sea Research (JSR), Elsevier, ff10.1016/j.seares.2014.03.004ff. ffhal-01248060, 2014

Parsons, D.R., Schindler, R.J., Hope, J.A., Malarkey,J., Baas, J.H., Peakall, J., Manning, A.J., Ye, J., Simmons, S., Paterson, D.M., Aspden, R.J., Bass, S.J., Davies, A.J., Lichtman, I.D., and Thorne, P.D.: The role of biophysical cohesion on subaqueous bed form size, Geophysical Research Letters, 43, 1566-1573, https://doi.org/10.1002/2016GL067667, 2016.

980   Paterson, D. M.: Short term changes in the erodibility of intertidal cohesive sediments related to the migratory behavior of epipelic diatoms, Limnology and Oceanography, 34, 223-234, https://doi.org/ 10.4319/LO.1989.34.1.0223, 1989.

Paterson, D. M., Yallop, M. L., and George, C.: Spatial variability in sediment erodibility on the island of Texel, BIS, Oldenburg, 1994.

Paterson, D. M.: Biological mediation of sediment erodibility: ecology and physical dynamics, in Cohesive Sediments, edited by N. Burt, Parker, R., Watts, J. (Eds.), pp. 215-230, Wiley Interscience, New York, 1997.

Paterson, D. M., Wiltshire, K. H., Miles, A., Blackburn, J., Davidson, I., Yates, M. G., McGrorty, S., and Eastwood:, J. A.: Microbiological mediation of spectral reflectance from intertidal cohesive sediments, Limnology and Oceanography, 43(6), 1207-1221, https://doi.org/10.4319/lo.1998.43.6.1207, 1998.

Paterson, D. M., Tolhurst, T. J., Kelly, J. A., Honeywill, C., de Deckere, E. M. G. T., Huet, V., Shayler, S. A., Black, K. S., de Brouwer, J., and Davidson, I.: Variations in sediment properties, Skeffling mudflat, Humber Estuary, UK, Continental Shelf Research, 20(10-11), 1373-1396, https://doi.org/ 10.1016/S0278-4343(00)00028-5, 2000.

Paterson, D. M., Hope J. A., Kenworthy J., Biles C. L., and Gerberdsdorf S. U.: Form, function and physics: the ecology of biogenic stabilisation. Journal of Soils and Sediments, https://doi.org/10.1007/s11368-018-2005-4, 18:3044–3054, 2018

Perkins, R., Honeywill, C., Consalvey, M., Austin, H. A., Tolhurst, T., and Paterson, D.: Changes in microphytobenthic chlorophyll a and EPS resulting from sediment compaction due to de-watering: Opposing patterns in concentration and content, Continental Shelf Research, 23, 575-586, https://doi.org/10.1016/S0278-4343(03)00006-2, 2003.

Pinckney, J. L.: A Mini-Review of the Contribution of Benthic Microalgae to the Ecology of the Continental Shelf in the South Atlantic Bight, Estuary and Coasts, 41, 2070-2078, https://doi.org/10.1007/s12237-018-0401-z, 2018

Pivato, M., Carniello, L., Gardner, J., Silvestri, S., and Marani, M.: Water and sediment temperature dynamics in shallow tidal environments: The role of the heat flux at the sediment-water interface, Advances in Water Resources, 113, 126-140, https://doi.org/10.1016/j.advwatres.2018.01.009, 2018.

Pivato, M., Carniello, L., Moro, I., and D'Odorico, P.: On the feedback between water turbidity and microphytobenthos growth in shallow tidal environments, Earth Surface Processes and Landforms, 44, 1192-1206, https://doi.org/ 10.1002/esp.4567, 2019.

Posey M. H., Alphin, T.D., Cahoon, L., Lindquist, D., and Becker, M. E.: Interactive effects of nutrient additions and predation on interfaunal communities, Estuaries, 22, 785-792, https://doi.org/10.2307/1353111, 1999.

Pratt, D. R., Pilditch, C. A., Lohrer, A. M., and Thrush, S. F.: The effects of short-term increases in turbidity on sandflat microphytobenthic productivity and nutrient fluxes, Journal of Sea Research, 92, 170-177, https://doi.org10.1016/j.seares.2013.07.009, 2014

Riethmüller, R., Heineke, M., Kühl, H., and Keuker-Rüdiger, R.: Chlorophyll a concentration as an index of sediment surface stabilisation by microphytobenthos? Continental Shelf Research, 20(10-11), 1351–1372. https://doi.org/10.1016/s0278-4343(00)00027-3, 2000

Righetti, M., and Lucarelli, C.: May the Shields theory be extended to cohesive and adhesive benthic sediments? Journal of Geophysical Research, Oceans, 112(C5), C05039. https://doi.org/10.1029/2006JC003669, 2007.

1015 Ruddy, G., Turley, C.M., and T.E.R. Junes. Ecological interaction and sediment transport on an intertidal mudflqat I. Evidence for a biologically mediated sediment-water interface, In: Black, K.S., Paterson, D.M., and A. Cramp (Eds.), Sedimentary Processes in the Intertidal Zone, Geological Society, London, Special Publication 139: 135-148, 1998.

Savelli, R., Dupuy, C., Barillé, L., Lerouxel, A., Guizien, K., Philippe, A., Bocher, P., Polsenaere, P., and Le Fouest, V.: On biotic and abiotic drivers of the microphytobenthos seasonal cycle in a temperate intertidal mudflat: A modelling study.
1020 Biogeosciences, 15(23), 7243–7271. https://doi.org/10.5194/bg-15-7243-2018, 2018

Savelli, R., Méléder, V., Cugier, P., Polsenaere, P., Dupuy, C., Lavaud, J., Barnett, A., and Le Fouest, V.: Mapping the Intertidal Microphytobenthos Gross Primary Production, Part II: Merging Remote Sensing and Physical-Biological Coupled Modeling. Front. Mar. Sci. 7:521. https://doi.org/10.3389/fmars.2020.00521, 2020

Schmidt, H., Thom, M., King, L., Wieprecht, S., and Gerbersdorf, S. U.: The effect of seasonality upon the development of
1025 lotic biofilms and microbial biostabilisation. Freshwater Biology, 61(6), 963–978. https://doi.org/10.1111/fwb.12760, 2016

Schmidt, H., Thom, M., Wieprecht, S., Manz, W., and Gerbersdorf, S. U.: The effect of light intensity and shear stress on microbial biostabilisation and the community composition of natural biofilms. Research and Reports in Biology 9: 1–16, https://doi.org/10.2147/RRB.S145282, 2018

Smith, D.J., and G.J.C. Underwood, 2000, The production of extracellular carbohydrates by estuarine benthic diatoms: the
1030 effects of growth phase and light and dark treatment, Journal of Phycology 36(2): 321-333.

Seminara, G., Lanzoni, S., Tambroni, N., and Toffolon, M.: How long are tidal channels?, J. Fluid Mech., 643, 479-494, https://doi.org/10.1017/S0022112009992308, 2010.

Shang, Q. Q., Fang, H. W., Zhao, H. M., He, G. J., and Cui, Z. H.: Biofilm effects on size gradation, drag coefficient and settling velocity of sediment particles. International Journal of Sediment Research, 29(4), 471–480,
1035 https://doi.org/10.1016/S1001-6279(14)60060-3, 2014.

Smith, N. P.: Observations and simulations of water-sediment heat exchange in a shallow coastal lagoon, Estuaries, 25(3), 483-487, https://doi.org/10.1007/BF02695989, 2002.

Spears, B., Saunders, J., Davidson, I., and Paterson, D.: Microalgal sediment biostabilisation along a salinity gradient in the Eden Estuary, Scotland: Unravelling a paradox, Marine and Freshwater Research, 59, 313, https://doi.org/10.1071/MF07164,
1040 2008.

Sutherland, T. F., Grant, J., and Amos, C. L.: The effect of carbohydrate production by the diatom Nitzschia curvilineata on the erodibility of sediment, Limnology and Oceanography, 43(1), 65-72, https://doi.org/10.4319/lo.1998.43.1.0065, 1998.

Tambroni, N., Bolla Pittaluga, M., and Seminara, G.: Laboratory observations on the morphodynamic evolution of tidal channels and tidal inlets, Journal of Geophysical Research, 110(F04009), https://doi.org/10.1029/2004JF000243, 2005.

1045 Tambroni, N., and Seminara, G.: A one-dimensional eco-geomorphoic model of marsh response to sea level rise: wind effects, dynamics of the marsh border and equilibrium. J. Geophys. Res. 117, F03026. https://doi.org/10.1029/2012JF002362, 2012.

Thom, M., Schmidt, H., Gerbersdorf, S. U., and Wieprecht, S.: Seasonal biostabilisation and erosion behavior of fluvial biofilms under different hydrodynamic and light conditions, International Journal of Sediment Research, 30, 271-284, https://doi.org/10.1016/j.ijsrc.2015.03.015, 2015.

1050   Thrush, S.F., Hewitt, J.E., and Lohrer, A.M.: Interaction networks in coastal soft-sediments highlight the potential for change in ecological resilience. Ecological applications 22, 1213-1223, https://doi.org/10.2307/23213955, 2012.

Todeschini, I., Toffolon, M., and Tubino, M.: Long-term morphological evolution of funnel-shape tide-dominated estuaries. J. Geophys. Res. 113, C05005. https://doi.org/10.1029/2007JC004094, 2008.

Tolhurst, T.J., Black, K.S., Paterson, D.M., Mitchener, H.J., Termaat, G.R., Shayler, S.A., 2000a. A comparison and
1055   measurement standardisation of four in situ devices for determining the erosion shear stress of intertidal sediments. Continental Shelf Research 20, 1397–1418. https://doi.org/10.1016/S0278-4343(00)00029-7

Tolhurst, T.J., Riethmüller, R., Paterson, D.M., 2000b. In situ versus laboratory analysis of sediment stability from intertidal mudflats. Continental Shelf Research 20, 1317–1334. https://doi.org/10.1016/S0278-4343(00)00025-X

Tolhurst, T. J., Gust, G., and Paterson, D. M.: The influence of an extracellular polymeric substance (EPS) on cohesive
1060   sediment stability, Fine Sediment Dynamics in the Marine Environment, 5, https://doi.org/10.1016/S1568-2692(02)80030-4, 2002.

Tolhurst, T. J., Black, K., and Paterson, D.: Muddy Sediment Erosion: Insights from Field Studies, Journal of Hydraulic Engineering, 135, https://doi.org/10.1061/(ASCE)0733-9429(2009)135:2(73), 2009.

Tolhurst, T. J., Defew, E. C., de Brouwer, J. F. C., Wolfstein, K., Stal, L. J., and Paterson, D. M.: Small-scale temporal and
1065   spatial variability in the erosion threshold and properties of cohesive intertidal sediments, Continental Shelf Research, 26(3), 351-362, https://doi.org/10.1016/j.csr.2005.11.007, 2006.

Uehlinger, U., Buhrer, H., and Reichert, P.: Periphyton dynamics in a floodprone prealpine river: Evaluation of significant processes by modeling, Freshwater Biol., 36, 249-263, https://doi.org/10.1046/j.1365-2427.1996.00082.x, 1996.

Underwood, G. J. C., and Paterson, D. M.: Seasonal changes in diatom biomass, sediment stability and biogenic stabilization
1070   in the Severn Estuary, Journal of the Marine Biological Association of the United Kingdom(73), 871-887, https://doi.org/10.1017/S0025315400034780, 1993.

Underwood, G. J. C., Paterson, D. M., and Parkes, R. J.: The measurement of microbial carbohydrate exopolymers from intertidal sediments, Limnology and Oceanography 40(7), 1243-1253, https://doi.org/10.4319/lo.1995.40.7.1243, 1995.

Underwood, G.J.C.. Adaptations of tropical marine microphytobenthic assemblages along a gradient of light and nutrient
1075   availability in Suva Lagoon, Fiji, European Journal of Phycology37(3): 449-462, 2002.

Valentine, K., and G. Mariotti. Repeated erosion of cohesive sediments with biofilms, Advances in Geosciences39: 9-14, 2014.

Van de Lageweg, W., McLelland S., and Parsons, D.: Quantifying biostabilisation effects of biofilm-secreted and synthetic extracellular polymeric substances (EPS) on sandy substrate. Earth Surface Dynamics Discussions. 1-37. https://doi.org/10.5194/esurf-2017-59, 2017.

1080 Van de Vijsel, R., van Belzen, J., Bouma, T. J., van der Wal, D., Cusseddu, V., Purkis, S. J., Rietkerk, M., and van de Koppel, J.: Estuarine biofilm patterns: Modern analogues for Precambrian self-organization, Earth Surface Processes And Landforms, 45, 1141-1154, https://doi.org/10.1002/esp.4783, 2020.

Vignaga, E., Sloan, D. M., Luo, X., Haynes, H., Phoenix, V. R., and Sloan, W. T.: Erosion of biofilm-bound fluvial sediments, Nature Geoscience, 6, 770-774, https://doi.org/10.1038/NGEO1891, 2013.

1085 Viparelli, E., Borhani, S., Torres, R., and Kendall, C. G. S. C. K.: Equilibrium of tidal channels carrying nonuniform sand and interacting with the ocean, Geomorphology, 329(2019), 1-16, https://doi.org/10.1016/j.geomorph.2018.12.017, 2019.

Viparelli, E., Sequeiros, O. E., Cantelli, A., Wilcock, P.R., and Parker, G.: River morphodynamics with creation/consumption of grain size stratigraphy 2: numerical model, Journal of Hydraulic Research, 48(6), 727-741, https://doi.org/10.1080/00221686.2010.526759, 2010.

1090 Walles, B., Paiva, J.S.de; van Prooijen, B. C.; Ysebaert, T., and Smaal, A. C.: The Ecosystem Engineer Crassostrea gigas Affects Tidal Flat Morphology Beyond the Boundary of Their Reef Structures. Estuaries and Coasts. 38. https:/doi.org/10.1007/s12237-014-9860-z, 2014.

Waqas, A., Neumeier, U., and Rochon, A.: Seasonal changes in sediment erodibility associated with biostabilisation in subarctic intertidal environment, St. Lawrence Estuary, Canada.Estuarine Coastal and Shelf Science 245(2):106935, 1095 https://doi.org/10.1016/j.ecss.2020.106935, 2020

Weerman, E. J., van de Koppel, J., Eppinga, M. B., Montserrat, F., Liu, Q., and Herman, P. M. J.: Spatial self-organization on intertidal mudflats through biophysical stress divergence. The American Naturalist, 176, E15–E32. https://doi.org/10.1086/652991, 2010

Weerman, E. J., Herman, P. M. J., and Van de Koppel, J.: Top-down control inhibits spatial self-organization of a patterned 1100 landscape, Ecology, 92(2), 487-495, https://doi.org/10.1890/10-0270.1, 2011a.

Weerman, E., Herman, P., and van de Koppel, J.: Macrobenthos abundance and distribution on a spatially patterned intertidal flat. Marine Ecology Progress Series, 440, 95–103. https ://doi.org/10.3354/ meps0 9332, 2011b

Widdows, J., Brinsley, M. D., Salkeld, P. N., and Lucas, C. H.: Influence of biota on spatial and temporal variation in sediment erodibility and material flux on a tidal flat (Westerschelde, The Netherlands), Marine Ecology Progress Series, 194, 23-37, 1105 https://doi.org/10.3354/meps194023, 2000.

Widdows, J., Friend, P. L., Bale, A. J., Brinsley, M. D., Pope, N. D., and Thompson, C. E. L.: Inter-comparison between five devices for determining erodability of intertidal sediments, Continental Shelf Research, 27(8), 1174-1189, https://doi.org/10.1016/j.csr.2005.10.006, 2007.

Wood, R., and Widdows, J.: A model of sediment transport over an intertidal transect, comparing the influences of biological and physical factors. Limnology and Oceanography 47, 848-855, https:doi.org/10.4319/lo.2002.47.3.0848, 2002.

Yallop, M., de Winder, B., Paterson, D. M., and Stal, L. J.: Comparative structure, primary production and biogenic stabilization of cohesive and non-cohesive marine sediments inhabited by microphytobenthos, Estuarine Coastal Shelf Science(39), 565-582, https://doi.org/10.1016/S0272-7714(06)80010-7, 1994a.

Yallop, M., de Winder, B., Paterson, D. M., and Stal, L. J.: Comparative structure, primary production and biogenic stabilization of cohesive and non-cohesive marine sediments inhabited by microphytobenthos, Estuarine Coastal Shelf Sci., 39, 565-582, https://doi.org/10.1016/S0272-7714(06)80010-7, 1994b.

Zhang, T., Tian, B., Wang, Y., Liu, D., Sun, S., Duan, Y., and Zhou, Y.: Quantifying seasonal variations in microphytobenthos biomass on estuarine tidal flats using Sentinel-1/2 data. Science of The Total Environment, 777, 146051. https://doi.org/10.1016/j.scitotenv.2021.146051, 2021.

Zhu, Q., van Prooijen, B. C., Maan, D. C., Wang, Z. B., Yao, P., Daggers, T., and Yang, S. L.: The heterogeneity of mudflat erodibility, Geomorphology, 345, https://doi.org/10.1016/j.geomorph.2019.106834, 2019.